2011
2012

GENEESKUNDE

*master in de biomedische wetenschappen: klinische moleculaire wetenschappen*

# Masterproef

## *Using stem cells as carriers of IL-4 to promote recovery after spinal cord injury*

Promotor :
Prof. dr. Sven HENDRIX
dr. Evi LEMMENS

Stefanie Lemmens

*Masterproef voorgedragen tot het bekomen van de graad van master in de biomedische wetenschappen , afstudeerrichting klinische moleculaire wetenschappen*

Maastricht University

universiteit hasselt
KNOWLEDGE IN ACTION



Universiteit Hasselt | Campus Diepenbeek | Agoralaan Gebouw D | BE-3590 Diepenbeek
Universiteit Hasselt | Campus Hasselt | Martelarenlaan 42 | BE-3500 Hasselt

2011
2012

# GENEESKUNDE

*master in de biomedische wetenschappen: klinische moleculaire wetenschappen*

# Masterproef

*Using stem cells as carriers of IL-4 to promote recovery after spinal cord injury*

Promotor :
Prof. dr. Sven HENDRIX
dr. Evi LEMMENS

Stefanie Lemmens

*Masterproef voorgedragen tot het bekomen van de graad van master in de biomedische wetenschappen , afstudeerrichting klinische moleculaire wetenschappen*

Maastricht University

universiteit hasselt
KNOWLEDGE IN ACTION

# Table of contents

**Table of contents** ..... **I**
**Acknowledgements** ..... **III**
**List of abbreviations** ..... **V**
**Summary** ..... **VII**
**Samenvatting** ..... **IX**
**1. Introduction** ..... **1**
1.2 Spinal cord injury ..... 1
1.2.1 Pathophysiology ..... 1
1.2.2 Spinal cord injury treatment ..... 2
1.3 IL-4 producing stem cells ..... 4
1.3.1 Interleukin-4 ..... 4
1.3.2 Stem cells ..... 6
1.4 Preliminary data ..... 7
1.5 Experimental approach ..... 8
**2 Materials and methods** ..... **11**
2.1 Cell cultures ..... 11
2.1.1 BMSCs ..... 11
2.1.2 NSCs ..... 11
2.1.3 *In vitro* differentiation of the NSC culture ..... 12
2.1.4 Primary neurons ..... 12
2.1.5 Astrocytes ..... 12
2.1.6 Fibroblasts ..... 12
2.1.7 Macrophages ..... 13
2.2 NSC phenotyping ..... 13
2.2.1 Immunofluorescence staining ..... 13
2.2.2 Fluorescence activated cell sorting ..... 14
2.3 Analyzing viability of the NSC culture after IL-4 treatment by MTT assay ..... 15
2.4 NSC proliferation assessment after IL-4 treatment by BrdU cell proliferation assay ..... 16
2.5 Real time-PCR to analyze IL-4 receptor expression ..... 16
2.6 Lentiviral vector transduction of BMSCs ..... 17
2.7 ELISA to quantify IL-4 expression by the transduced BMSCs ..... 17
2.8 Animal experiments ..... 17
2.8.1 BMSC transplantation in the SCI hemisection mouse model ..... 17
2.8.2 Behavioral analysis ..... 18
2.8.3 Analysis of spinal cord tissue sections by histology ..... 18
2.9 Statistical analysis ..... 19
**3 Results** ..... **21**
3.1 Isolation, culture and *in vitro* characterization of NSCs from BALB/c-mice ..... 21

3.1.1 NSCs express A2B5, NCAM, GFAP, BLBP and SOX2, but are negative for CD45, Sca-1, Tuj1 and NeuN ..... 22
3.1.2 NSCs have the capacity to differentiate into glial and neuronal cell lineages *in vitro* ..... 24
3.2 Effect of recombinant mouse IL-4 treatment on the phenotype of NSCs *in vitro* ..... 26
3.2.1 MTT assay indicates no effect on viability of NSCs treated with different concentrations of recombinant mouse IL-4 ..... 26
3.2.2 BrdU cell proliferation assay indicates no effect on proliferation of NSCs treated with different concentrations of recombinant mouse IL-4 ..... 27
3.2.3 Addition of 5 ng/ml IL-4 to differentiating NSCs significantly increases their differentiation into neurons, with additional significant increase in neurite length ..... 28
3.3 IL-4 receptor component expression on NSCs ..... 30
3.3.1 Real-time PCR suggests the expression of IL-13Rα1 on the NSCs after quantitative analysis and expression of IL-13Rα1 and IL-2Rγ after gel electrophoresis, however expression of IL-4Rα is also suggested after IL-4 treatment ..... 30
3.3.2 The NSCs show immunoreactivity for IL-13Rα1 ..... 32
3.4 Culture and characterization of BALB-c BMSCs expressing eGFP, luciferase and IL-4 ..... 33
3.4.1 The BMSCs secrete IL-4 in the culture medium after transduction ..... 33
3.5 Transplantation of IL-4 producing BMSCs after SCI ..... 34
3.5.1 Transplantation of IL-4 producing BMSCs does not significantly improve functional outcome after SCI ..... 34
3.5.2 Immunofluorescence and histological analysis does not reveal the presence of transplanted BMSCs at the lesion site, three weeks after transplantation ..... 35
**4 Discussion ..... 37**
4.1 Isolation, culture and *in vitro* characterization of NSCs from BALB/c-mice ..... 37
4.2 Effect of recombinant mouse IL-4 treatment on the phenotype of neural stem cells *in vitro.* ..... 38
4.3 IL-4 receptor subunit expression on NSCs ..... 39
4.4 Culture and characterization of BALB-c BMSCs expressing eGFP, luciferase and IL-4 ..... 42
4.5 Transplantation of IL-4 producing BMSCs after SCI ..... 42
**5 Conclusion ..... 47**
**References ..... 49**
**Supplemental information ..... 55**

# Acknowledgements

Eight months ago, I started the internship which resulted in this thesis. The practical training and the thesis would not be possible without the help and support of several people. Therefore, I would like to use this preface to thank everybody who helped me during my internship.

First of all, I would like to thank my promoter Prof. Dr. Sven Hendrix for the opportunity to perform my internship in his research group. I want to thank him for the trust, responsibility and freedom to work at my thesis project, which resulted in a very instructive internship. With his guidance and critical view, I learned how to perform research independently and in group. However, becoming a skilled researcher would not be possible without the help of the other members of Morphology. Therefore, I would like to thank my co-promoter Dr. Evi Lemmens, as well as Dr. Nathalie Geurts, Ir. Sofie Nelissen, Tim Vangansewinkel, Pia Vidal Vera, Dr. Annelies Bronckaerts, Dr. Wendy Martens, Petra Hilkens, Pascal Gervois and Monika Broeders. Furthermore, special thanks to my daily supervisor Dearbhaile Dooley for her support, expertise and guidance.

I also want to thank my second examiner Dr. Leen Slaets for her advice and suggestions during this project and for critical reviewing my thesis. For advice and providence of stem cells and vectors, I would like to thank Dr. Peter Ponsaerts and Dr. Kristien Reekmans (Laboratory of Experimental Hematology, Vaccine, and Infectious Disease Institute, University of Antwerp).

Lastly, thanks to my fellow students, friends and family for the support, not only during this year, but during my whole education.

# List of abbreviations

| | |
|---|---|
| 7-AAD | 7-aminoactinomycin D |
| MTT | 3-(4,5-dimethylthiazol-2-yl)-2,5-diphenyl tetrazolium bromide |
| Arg-I | Arginase-I |
| BMS | Basso Mouse Scale |
| Tuj1 | Beta-III tubulin |
| BLI | Bioluminescence imaging |
| BDA | Biotinylated dextran amine tracing |
| BMSCs | Bone marrow stromal cells |
| BLBP | Brain lipid binding protein |
| BDNF | Brain-derived neurotrophic factor |
| BrdU | Bromodeoxyuridine |
| CCR5 | C-C chemokine receptor type 5 |
| CNS | Central nervous system |
| CST | Corticospinal tract |
| CXCR4 | C-X-C Chemokine receptor type 4 |
| DMSO | Dimethylsulfoxide |
| eGFP | enhanced Green Fluorescent Protein |
| ELISA | Enzym linked immunosorbent assay |
| FCS | Fetal calf serum |
| Fluc | Firefly luciferase |
| FACS | Fluorescence activated cell sorting |
| gDNA | Genomic DNA |
| GFAP | Glial fibrillary acidic protein |
| HBSS | Hank's Buffered Salt Solution |
| HE | Hematoxilin and Eosin |
| hEGF | Human epidermal growth factor |
| hFGF-2 | Human fibroblast growth factor-2 |
| HS | Horse serum |
| Iba-1 | Ionized calcium binding adaptor molecule-1 |
| ICC | Immunocytochemistry |
| IHC | Immunohistochemistry |
| IFN-γ | Interferon gamma |
| IL-13 | Interleukin-13 |
| IL-13Rα1 | Interleukin-13 receptor alpha 1 |
| IL-13Rα2 | Interleukin-13 receptor alpha 2 |
| IL-4 | Interleukin-4 |
| IL-4Rα | Interleukin-4 receptor alpha |
| IMDM | Iscove's Modified Dulbecco's Medium |
| Jaks | Janus family of protein kinases |
| LV | Lentiviral |
| LPS | Lipopolysaccharide |
| LFA-1 | Lymphocyte function associated antigen-1 |
| MSCs | Mesenchymal stem cells |
| NCAM | Neural cell adhesion molecule |
| NDM | Neural differentiation medium |
| NEM | Neural expansion medium |
| NSCs | Neural stem cells |
| NeuN | Neuronal Nucleus |
| PFA | Paraformaldehyde |
| P/S | Penicillin/Streptomycin |
| PBS | Phosphate buffered saline |
| PDL | Poly-D-lysine |
| PLL | Poly-L-lysine |
| PURO | Puromycin |
| qPCR | Quantitative PCR |
| ROS | Reactive oxygen species |
| RT | Room temperature |
| RPMI | Roswell Park Memorial Institute medium |
| SOX2 | Sex determining region Y-box 2 |
| SCI | Spinal cord injury |
| SD | Standard deviation |
| SEM | Standard error of the mean |
| Sca-1 | Stem cell antigen-1 |
| SCs | Stem cells |
| SVZ | Subventricular zone |
| Th2 | T helper 2 |
| TGF-β1 | Transcription growth factor-β1 |
| TNF-α | Tumor necrosis factor-α |
| Tuj1 | Beta-III tubulin |

# Summary

Spinal cord injury (SCI) is a devastating disease for which no curative therapy is available. Spontaneous regeneration of the central nervous system (CNS) is limited, due to intrinsic inhibition of neuroregeneration, but also resulting from SCI-associated inflammation. Therefore, research on new therapeutic strategies focuses on modulation of this inflammatory response.

Bone marrow stromal cells (BMSCs) and neural stem cells (NSCs) have been reported to secrete trophic factors, induce axonal sprouting and improve functional outcome after SCI. Furthermore, they possess immunomodulatory properties via the secretion of cytokines and chemokines. The cytokine interleukin-4 (IL-4) is of special interest because beneficial effects of IL-4 after CNS injury have been previously reported, by polarization of the immune response to anti-inflammatory and by enhancing neural proliferation, survival and neuronal differentiation. Preliminary data of our research group have shown that IL-4 promotes regeneration and functional recovery after SCI. Therefore, stem cells (SCs) secreting IL-4 could be a promising therapeutic strategy combining immunomodulation via IL-4 and the benefits of SC transplantation.

The Master thesis project falls within the scope of a larger PhD-project that investigates the use of SCs as carriers of IL-4 to promote recovery after SCI. In the thesis project transplantation of IL-4 secreting bone marrow stromal cells (BMSCs) was used for the 'proof of principle', while the NSCs were characterized and transduced for their use in future experiments.

In the first part of this study, isolated NSCs were characterized by their expression of the markers GFAP, BLBP, SOX2, A2B5 and NCAM and their differentiation potential into glial and neuronal cell lineages *in vitro*. Next, the effect of recombinant mouse IL-4 treatment on the phenotype of NSCs was investigated *in vitro*. MTT assay and BrdU assay indicated no significant differences in survival or proliferation between NSCs treated with different IL-4 concentrations. However, low concentrations of IL-4 significantly increased neuronal differentiation and neurite length when added to a differentiating NSC-culture. Besides indirect effects of IL-4 on regeneration, e.g. via macrophage polarization, several reports also suggest direct effects of IL-4. Therefore, IL-4 receptor component expression on the NSCs was investigated by real-time PCR, combined with gel electrophoresis and immunocytochemistry (ICC). The results suggested expression of IL-13Rα1 and IL-2Rγ. Furthermore, when the NSCs were treated with IL-4, expression of IL-4Rα, next to IL-13Rα1 and IL-2Rγ, was also suggested. However, these results need further confirmation.

Secondly, a pilot study with BMSCs was performed to investigate whether the use of SCs is a good way of delivering IL-4 to the site of injury, continuously, at a low concentration. After confirmation of IL-4 expression by the transduced BMSCs *in vitro*, transplantation was performed in the hemisection SCI mouse model. Functional tests did not indicate a significant difference in functional recovery between the animals, transplanted with the IL-4 transduced BMSCs, and the control groups, treated with BMSCs or PBS. Therefore, further research is needed to reveal the therapeutic potential of transplanted stem cells as carriers for the local delivery of anti-inflammatory cytokines to improve recovery after spinal cord injury.

# Samenvatting

Ruggenmergletsels (SCI) zijn ernstige aandoeningen waarvoor nog geen curatieve therapie beschikbaar is. Spontane regeneratie van het centrale zenuwstelsel (CZS) is beperkt, door de intrinsieke remming van neuroregeneratie, maar ook door ruggenmergletsel-geassocieerde inflammatie. Daarom is onderzoek naar nieuwe therapeutische strategieën vooral gericht op modulatie van deze ontstekingsreactie.

Van beenmerg stromale cellen (BMSC) en neurale stamcellen (NSC) is gekend dat ze trofische factoren secreteren, en axonale uitgroei en functioneel herstel na SCI bevorderen. Bovendien bezitten ze immuunmodulerende eigenschappen door de secretie van chemokines en cytokines. Vooral interleukine-4 (IL-4) is interessant; dit cytokine stimuleert herstel na CZS-letsels, leidt tot polarisatie van de immuunrespons naar anti-inflammatoir en bevordert neuronale proliferatie, overleving en differentiatie. Bovendien heeft onze onderzoeksgroep aangetoond, dat IL-4 regeneratie en functioneel herstel bevordert na ruggenmergschade. Door de combinatie van de immuunmodulerende eigenschappen van IL-4 met de vermelde voordelen van stamceltransplantatie, zijn IL-4 secreterende stamcellen (SC) mogelijk een veelbelovende therapeutische strategie voor CZS-letsels.

Het Master thesis-project valt binnen het kader van een groter PhD-project, dat onderzoek verricht naar het gebruik van SC als dragers van IL-4, om herstel na SCI te bevorderen. In het thesisproject werden IL-4 secreterende BMSC getransplanteerd om dit principe te onderzoeken, terwijl de NSC gekarakteriseerd en getransduceerd werden voor gebruik in toekomstige experimenten.

In het eerste deel van deze studie, werden de geïsoleerde NSC gekarakteriseerd door hun expressie van de merkers GFAP, SOX2, BLBP, A2B5 en NCAM en hun differentiatiepotentieel in gliale en neuronale cellijnen *in vitro*. Vervolgens werd *in vitro* het effect van recombinant muis-IL-4 op het fenotype van deze NSC onderzocht. MTT en BrdU assay toonden geen effect van IL-4 op de overleving of proliferatie tussen NSC. In tegenstelling, lagere concentraties van IL-4 bevorderden neuronale differentiatie, gepaard met een significante stijging in de lengte van de neurieten.

Naast indirecte effecten van IL-4 op regeneratie, bv. via macrofaag polarisatie, werden eerder ook directe effecten gerapporteerd. Daarom werd in dit thesisproject de expressie van IL-4 receptor componenten op NSC onderzocht door real-time PCR, gecombineerd met gel elektroforese en immunocytochemie (ICC). De resultaten suggereerden expressie van IL-13Rα1 en IL-2Rγ. Bovendien vertoonden NSC, behandeld met IL-4, ook expressie van IL-4Rα. Echter, deze resultaten moeten nog worden bevestigd.

Ten tweede werd er een pilootstudie met BMSC uitgevoerd, om te onderzoeken of het gebruik van SC een goede manier is om IL-4, continu en in een lage concentratie, aan te leveren op de plaats van het letsel. Na bevestiging van IL-4 expressie door de getransduceerde BMSC *in vitro*, werden deze getransplanteerd in een muismodel voor ruggenmergletsels. Functionele testen duidden niet op een significant verschil in herstel tussen de dieren, getransplanteerd met IL-4 getransduceerde BMSC, en de controle groepen, behandeld met BMSC of PBS. Er is dus nood aan verder onderzoek om het therapeutisch potentieel van getransplanteerde SC, als dragers voor de lokale levering van anti-inflammatoire cytokines om herstel na ruggenmergletsels te verbeteren, te bevestigen.

# 1. Introduction

## 1.2 Spinal cord injury

Spinal cord injury is a devastating disease, leading to the loss of motor, sensory and autonomous functions below the lesion site. The spinal cord consists of a bundle of nervous tissue which conducts motor and sensory information to and from the brain and coordinates reflexes. Transverse sections of the spinal cord show the relationship between white and gray matter (1). The peripheral situated white matter tracts contain myelinated motor and sensory axons. The cell bodies of the sensory neurons are contained within dorsal root ganglia. The central gray matter consists of the cell bodies of interneurons and motor neurons. In the context of SCI the corticospinal tract (CST), situated in the left and right dorsal funiculus and the ventral funiculus of the white matter, receives special attention because this tract mediates voluntary control of limb movements (2).

SCI has an enormous impact in an individual-familial and socio-economic context, partly due to the young mean age (33 years) of the patients. The life-long supportive care to prevent several complications means a substantial financial burden (200 000EUR/patient/year) for both patients and society (3). Initial trauma can be caused by working accidents (28%), motor vehicle accidents (24%) and sporting and recreation accidents (16%) (Christopher and Dana Reeve foundation 2011, www.christopherreeve.org).

### 1.2.1 Pathophysiology

The initial mechanical trauma (primary injury, figure 1A) can result in contusion, compression, penetration or maceration of the spinal cord, with blood vessel damage, disruption of axons and damage to neural cell membranes as a consequence. These primary events are followed by secondary injury (figure 1A) which includes ischemia, glutamatergic excitotoxicity, free radical formation and inflammation (1, 4).

Disruption of the vasculature, the resulting ischemia and other disturbances of the cellular metabolism cause energetic failure, which disturbs membrane polarization through ionic transporters since the maintenance of membrane polarization is an energy-intensive cellular process. The inability of neurons to maintain their membrane polarization makes them more easily excitable and makes them release excitatory transmitters, such as glutamate. Moreover, ischemia, combined with reoxygenation via reperfusion and the excitotoxic neurons, leads to an excess in reactive oxygen species (ROS). These events result in an array of pathological effects such as the degradation of proteins and membranes, a decrease in cellular survival, calcium-induced mitochondrial dysfunction, axon demyelination and the alteration of blood-brain barrier permeability, which in turn mediates increased recruitment of inflammatory cells (5, 6). Furthermore, peak periods of infiltration of inflammatory cells coincidence with angiogenesis and glial scar formation (figure 1B) (7).

Key players in the inflammation reaction after SCI are microglia and astrocytes, which regulate the immune response in the CNS.

Their activation leads to an increase in the release of cytokines and chemokines and the expression of adhesion molecules, which in turn facilitate the adhesion, migration and extravasation of inflammatory cells (e.g. macrophages, neutrophils, T-cells) to the site of injury.

The described secondary injury results in the formation of glial scar tissue surrounding a central cavitation (figure 1A), which is a physical and chemical barrier for endogenous regeneration (4). The failure of regeneration and the disruption of descending and ascending axonal tracts by the scar tissue and cavitation, lead to the loss of sensory and motor function (1).

Molecules associated with the glial scar (e.g. chondroitin sulfate proteoglycans) further inhibit axonal regeneration. Other inhibitors are associated with myelin (e.g. Nogo-A) and the extracellular matrix (2, 4, 6) (**extrinsic** adult CNS barriers). Furthermore, the inflammation after SCI is a source of cytokines and other signaling molecules which upregulate inhibitory molecules (8). The loss of an **intrinsic** ability to overcome this inhibition in neurons and the lack of trophic support also contribute to the failure of regeneration (9, 10). All together, the failure of axons to regenerate, results from decreased intrinsic properties of the neurons, the absence of neurothrophic factors and the presence of inhibitory factors in the environment.

The inflammatory cascade after SCI is an attempt to restore homeostasis via the elimination of pathogens and the removal of damaged cells, but it causes deleterious effects on the surrounding healthy tissue due to the release of toxic substances (6). However, next to these detrimental consequences, beneficial effects are also reported (11), like inflammation-produced factors that stimulate neurogenesis and oligodendrogenesis (e.g. interleukin-4) (12). Therefore, modulation of the inflammatory response after SCI could be a promising strategy for future efficient treatment.

### 1.2.2 Spinal cord injury treatment

Despite major progress in pharmacological and surgical treatments, there is currently no existing curative therapy for SCI (4). The current therapeutic intervention focuses on prevention and restriction of secondary inflammatory responses in the acute stage. This is achieved by decompression of the spinal cord by laminectomy to limit ischemia, by orthopedic fixation of the involved vertebra to limit extra damage by bone pieces and by administration of high doses of steroids (methylprednisolone) to limit edema formation. However, this current treatment modality provides only modest efficacy, especially in chronic stages of SCI (13).

For a future efficient treatment, four main approaches can be considered: tissue or cell transplantation, providing growth stimulating factors (neurotrophic factors), blocking factors which inhibit neural regeneration, and modulating the inflammatory response (figure 1A) (4).

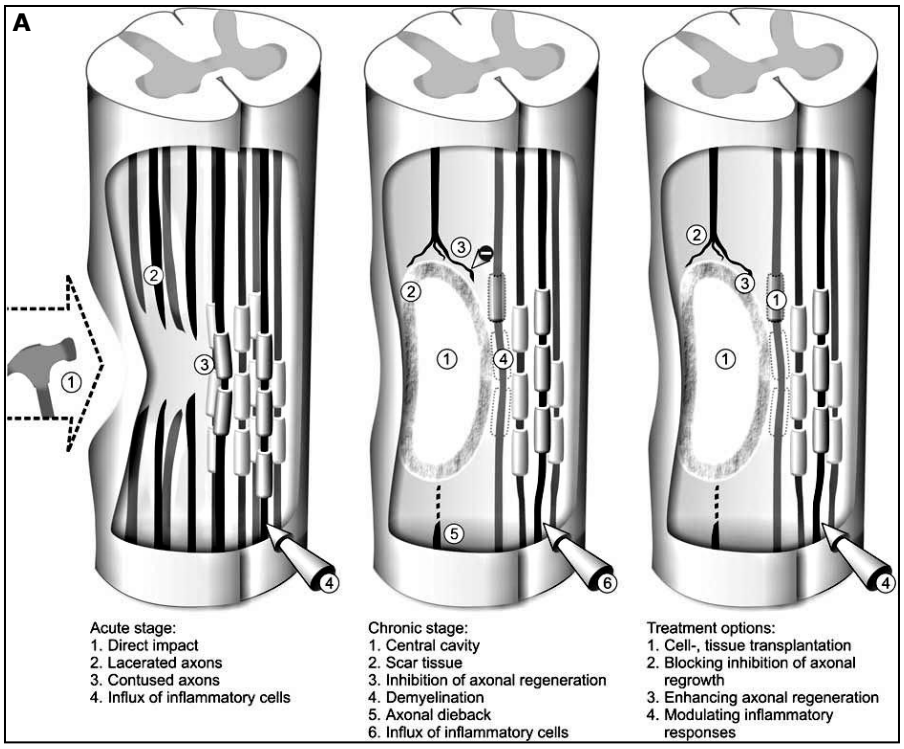


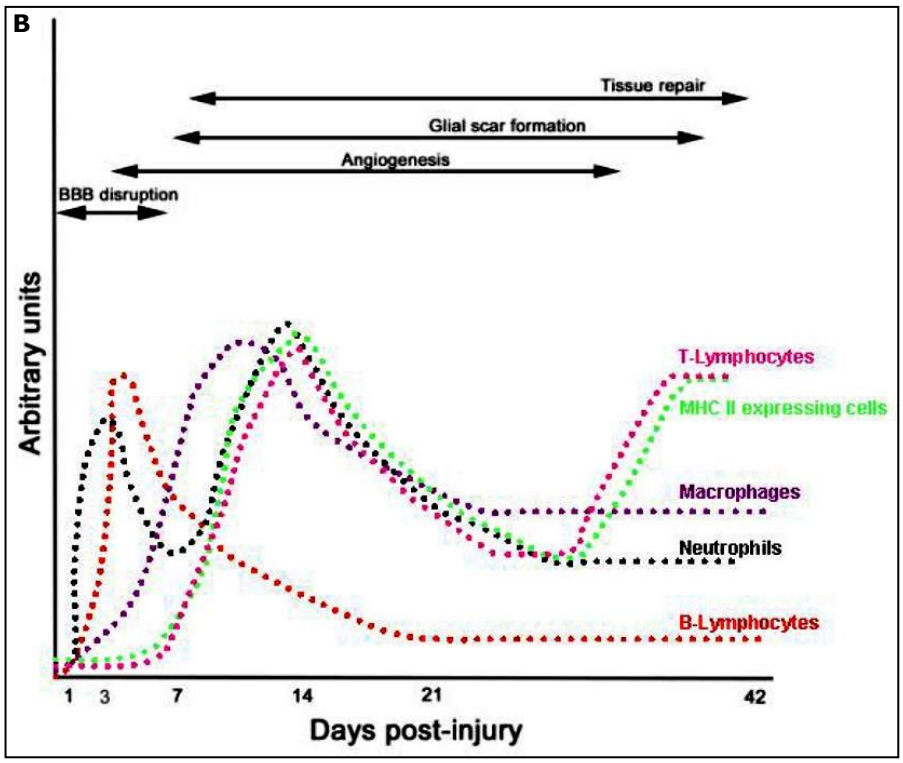


**Figure 1: The pathophysiological process of SCI. A)** The acute and chronic phase are depicted. The different treatment options are also indicated (Ronsyn *et al*, Spinal Cord 2009). **B)** This figure illustrates the timing of infiltration of inflammatory cells in relation to secondary pathogenesis and wound healing (Trivedi *et al*, Clin Neurosc Res. 2006).

## 1.3 IL-4 producing stem cells

In this project, transplantation of IL-4-secreting stem cells has been used to combine two approaches, namely immunomodulation via IL-4 and SC-transplantation. IL-4 was chosen because several reports suggest its indirect positive effect on regeneration after SCI, by polarization of the spinal cord micro-environment to anti-inflammatory (T helper 2 (Th2) response). SCs, more specifically NSCs and BMSCs, were used as carriers IL-4, to deliver the cytokine continuously to the site of injury. Besides their function as carriers, SCs in SCI have been reported as being beneficial because they may contribute to functional recovery by the formation of myelin and by the promotion and guidance of axonal growth (14). Furthermore, SCs can be used to bridge the site of injury or for trophic support contributing to plasticity in the spared spinal cord (14).

### 1.3.1 Interleukin-4

IL-4 is a Th2 cytokine with diverse functions, including co-stimulation of growth as well as promotion of survival of cultured T and B cells, differentiation of T lymphocytes to the Th2 phenotype and down-regulation of pro-inflammatory functions of monocytes and macrophages (15). Moreover, IL-4 has been reported to enhance the death of activated microglial cells and it inhibits autophagy responses (15). IL-4 shares a common receptor component with interleukin-13 (IL-13), namely the IL-4 receptor alpha (IL-4Rα) chain, which is responsible for signal transduction via downstream pathways that mediate gene expression, cell proliferation and survival (figure 2)(16).

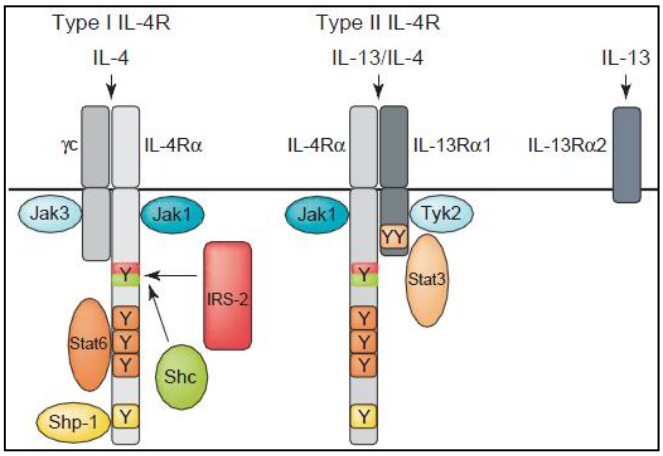


**Figure 2: Schematic illustration of the IL-4 and IL-13 receptor complexes.** The type I IL-4R consists of the IL-4Rα chain and the γc chain. This receptor complex binds exclusively IL-4 and predominates in hematopoietic cells. The type II IL-4R complex consist of IL-4Rα and interleukin-13 receptor alpha 1 (IL-13Rα1). This complex binds IL-4 and IL-13. It is expressed on hematopoietic and non-hematopoietic cells. The IL-13 receptor alpha 2 (IL-13Rα2) chain exclusively binds IL-13 and serves as a decoy receptor. Subunits of the receptor complexes are associated with the Janus family of protein kinases (Jaks) and downstream pathways that mediate gene expression, proliferation and cell survival (Chatila, TRENDS in Molecular Medicine 2004).

## IL-4 after SCI

The expression of IL-4 and its receptor have previously been shown to be acutely increased after SCI. This endogenous IL-4 may control post-injury inflammation and secondary degenerative processes by regulating early macrophage activation, as indicated by a neutralization experiment (17). IL-4 guides macrophage polarization to alternatively activated M2-macrophages, which are involved in angiogenesis, matrix remodeling and suppressing destructive immunity (18). This is in contrast to classically activated M1 macrophages, which are involved in host defense but also cause collateral damage to healthy tissue (18). The polarization to M2 macrophages has been reported to promote repair and to block secondary injury. Furthermore, depletion of macrophages is neuroprotective and promotes functional recovery, probably because microglia and newly recruited monocytes differentiate into pro-inflammatory M1-macrophages at sites of SCI (18).

Kuo *et al* confirmed the beneficial effects of M2 macrophage polarization, caused by IL-4 expression. They suggested that T cells, infiltrating the lesion site 3-7 days after SCI, may contribute to this IL-4 expression. After a peripheral nerve graft (6-14 days), a delayed but persistent induction of Th2 cytokines was found which resulted in a Th2 shift of the immune response. The Th2 shift, in turn, lead to an M2 macrophage response, implied to play an important role in axonal regeneration (19).

Other reports also state that Th2 cells are particularly beneficial in the context of CNS lesions (20). Kiyota *et al* showed that CNS expression of IL-4 can directly enhance neurogenesis, likely by enhancing neural progenitor cell proliferation and neuronal differentiation. The mechanisms by which IL-4 induced proliferation include, activation of extracellular signaling-regulated kinases, insulin-response 1 and 2 pathways and the activation of phophatidylinositol-3-kinase and Akt, protecting neurons from apoptosis (21). Derecki *et al* showed that meningeal T cell-derived IL-4 antagonized the deleterious effects of pro-inflammatory cytokines on astrocytes and neurons and it promoted the expression of an astroglial phenotype producing BDNF (22). Furthermore, IL-4 also exerts neuroprotective effects via the regulation of free radical formation (23).

All together these reports suggest a beneficial effect of IL-4 after CNS injury by polarization of the immune response to Th2, by an increase in M2 macrophages and by enhancing neural proliferation, survival and neuronal differentiation.

## IL-4 and stem cell therapy

An autocrine effect of IL-4 on the SCs may be observed, provided they possess the IL-4 receptor (direct effect). However, the expression of the IL-4 receptor on NSCs has not yet been reported and needs further investigation, although the literature suggests direct effects. A reported effect of IL-4 treatment on NSCs is the upregulation of surface adhesion molecule lymphocyte function associated antigen-1 (LFA-1) and the chemokine receptors C-X-C chemokines receptor type 4 (CXCR4) and C-C chemokines receptor type 5 (CCR5). This indicates that the use of the IL-4 may facilitate the migration of the NSCs into CNS inflammatory sites, producing stronger therapeutic effects (24).

On cloned stromal cell lines from the bone marrow the IL-4 receptor was found (25), but the expression on the provided BMSCs, isolated from BALB/c mice, needs to be confirmed.

Furthermore, direct effects of IL-4 on BMSCs have not been reported, although Payne *et al* state that the transduction of adipose derived mesenchymal stem cells (MSCs) with IL-4 and enhanced Green Fluorescent Protein (eGFP) did not change the expression of homing molecules (26).

### 1.3.2 Stem cells

SCs can be defined as self-renewing, multipotent or pluripotent progenitors with the broadest developmental potential in a particular tissue at a particular time (27). Besides self-renewal, also proliferation, the production of a large number of differentiated functional progeny, and regenerating the tissue after injury, characterize stem cells (28). However, the microenvironment, including the surrounding cells, the extracellular matrix and the local milieu with growth and differentiation factors, also determines the SC-function (29).

SC-therapy after SCI may contribute to functional recovery by replacement of damaged neural tissue and by bystander mechanisms, such as trophic support to endogenous neural regeneration and immunomodulation.

#### Neural stem cells

The injured and degenerating CNS initially attempts to repair damaged neural tissue, as demonstrated by an increase in proliferation of subventricular zone (SVZ)-NSCs. However, endogenous repair mechanisms are insufficient to achieve substantial functional recovery. Therefore, NSC transplantation might have the potential to regenerate tissue by replacing the cells that are lost during damage or disease. NSCs can also exert a beneficial effect on neuroregeneration by trophic support and by changing the inflammatory spinal cord-micro-environment after SCI. This immunomodulation can be extra stimulated by genetic modification of the NSCs to express immune-signaling cytokines. In this way, the SCs become therapeutic vehicles to deliver factors or proteins. Moreover, NSCs are highly migratory and seem to be attracted to areas of brain pathology, which is an ideal characteristic for their use as delivery vehicles (30). Another advantage of NSCs is that they have the potential to integrate seamlessly into the host brain without disrupting normal function (30).

Stem cell therapy after SCI is promising but as a mono-therapy maybe insufficient, because the regeneration and functional recovery after NSC transplantation are mostly reported as temporary (14). Multiple studies showed a limited survival and differentiation potential of engrafted stem cells, because the inflammatory environment alters self-renewal, survival, migration and differentiation of the NSCs (14). Reekmans *et al* have shown that the NSCs survive for two weeks after engraftment into the uninjured brain and histology indicated differentiation into astrocytes ($GFAP^+$), but not into neurons ($Tuj^+$), after transplantation (31). Therefore, we combine SC-therapy with IL-4 treatment to create a more permissive environment, aiming to prolong NSC survival and to promote neuronal differentiation *in vivo*.

#### Bone marrow stromal cells

While characterizing and preparing IL-4 secreting NSCs for transplantation, BMSCs were used in the mean time for the 'proof of principle', namely that the use of SCs as carriers of IL-4 improves functional outcome.

The BMSCs were used in a parallel project that investigates the rejection of transplanted cells by the microglia/macrophage response in the healthy brain. Therefore, the SCs were already characterized having the BMSC-identity, were lentivirally transduced with the eGFP and Firefly luciferase (Fluc) reporter genes and were single cloned.

BMSCs from BALB/c-mice are characterized by their expression of V-CAM and MHC-I, without the detectable expression of hematopoietic (CD45, c-kit, MHC-II), endothelial (CD31) and neural (A2B5) membrane proteins (32, 33). However, there is a variable expression of markers used to identify BMSCs due to variation in tissue source, the method of isolation and culture, and species differences (34). The other identification criteria, besides the expression or the lack of certain surface molecules, are plastic-adherence in standard culture conditions and differentiation in osteoblasts, adipocytes and chondroblasts *in vitro* (35).

Although NSCs are preferred in this study, because they may possess intrinsic properties that are superior to BMSCs (e.g. differentiation into oligodendrocytes and neurons and integration into the CNS tissue without disturbing function) (30, 34, 36, 37), BMSCs were previously used to investigate their transplantation in animal models of SCI. The reported beneficial effects after their transplantation were remyelination, axonal outgrowth and improved locomotion (38-40). BMSCs alter the tissue microenvironment via the secretion of soluble factors which may contribute more significantly than their capacity for transdifferentiation into neurons (41). They establish an environment permissive for axon regeneration via the secretion of neurotrophic cytokines, the synthesis of nerve permissive matrix elements and the formation of bridges (guidance strands) (38-40). A study by Nakajima *et al* has shown that BMSC transplantation changes the spinal cord microenvironment with a shift in the macrophage phenotype (M1→M2), an increase in IL-4 and IL-13, and a decrease in tumor necrosis factor alpha (TNF-α) and interleukin-6 (IL-6) (40). These changes lead to improved preservation of axons and myelin sparing, to less scar tissue formation and to improved functional locomotion recovery (40). Other advantages of BMSCs are, that they are not ethically restricted and have a low immunogenicity (allogeneic)(42). Moreover, they represent an ideal stem cell source because of their easy isolation (bone marrow biopsies), purification and amplification (32, 43).

## 1.4 Preliminary data

Neural stem cell-based gene therapy in animal models has only been used in studies on Alzheimer's disease, injury-induced neuropathic pain and brain malignancy (30). NSCs expressing IL-4 have been used for the treatment of brain tumors (44). The results of this study showed that neural progenitor cells, engineered to release high levels of IL-4, have a strong anti-tumor effect and are more effective than retrovirus-mediated *in vivo* transfer of IL-4 (44). It was concluded that the anti-tumorigenic effects of the NSCs were down to their lower susceptibility to immune rejection in comparison to the retroviral delivery method, their migratory capacity as well as the release of anti-proliferative factors (44).

The use of BMSCs as gene delivery vehicles has been applied multiple times to attenuate arthritis (45), for cancer therapy (46-52) and to prevent lung ischemia-reperfusion injury (53), but there are no reports on SCI.

IL-4 overexpressing MSCs were recently used to intervene in experimental autoimmune demyelination, with reported improvement of anti-inflammatory responses and functional recovery (26).

Previous results from our research group suggested that IL-13 is a potent promoter of axonal regeneration *in vitro*, which occurs independent from neuronal cell survival (54). Other results indicated that acute treatment with recombinant IL-4 significantly promotes functional recovery after SCI, while IL-13 exerts opposing effects and thus impairs clinical outcome after SCI *in vivo* (55). IL-4 improves locomotion restoration from day 1 after operation, as revealed by the Basso Mouse Scale (BMS) and the Rotarod performance test (55). Histological analysis showed that IL-4 stimulates axon regrowth in the lesioned spinal cord *in vivo* (55). IL-4 and IL-13 were delivered locally to the lesion (55). As a clinical application, this method is not ideal due to the possible side-effects associated with immunogenicity (1). Furthermore, stem cell therapy could have additional positive effects like production of trophic factors or secretion of more physiological concentrations of identified factors (e.g. transgenes). Therefore, we investigate whether IL-4-secreting NSCs/BMSCs are a good way to deliver IL-4 to the site of injury to improve outcome. The aim of the project is to improve functional outcome by changing the spinal cord micro-environment to anti-inflammatory and by promoting survival of the stem cells, with the use of IL-4.

## 1.5 Experimental approach

In the first part of this study, isolated NSCs were characterized for the expression of different neural markers by Fluorescence activated cell sorting (FACS) and ICC. The **NSC identity** was further revealed by their differentiation potential. After *in vitro* differentiation, ICC was used to investigate the expression of glial and neuronal markers. Next, the presence of IL-4 receptor units on the NSCs was determined by real time polymerase chain reaction (quantitative PCR, qPCR), to reveal possible autocrine effects of IL-4. The **effect of recombinant mouse IL-4 on the NSC phenotype *in vitro*** was investigated by 3-(4,5-dimethylthiazol-2-yl)-2,5-diphenyl tetrazolium bromide (MTT) assay, bromodeoxyuridine (BrdU) cell proliferation assay and a differentiation assay followed by ICC and cell counting.

In the second part of the project, a pilot study with BMSCs has been performed **to investigate whether the use of SCs are a good way to deliver IL-4 to the site of injury, continuously, at a low concentration**. In the meanwhile, the characterized NSCs were lentivirally transduced with the reporter genes eGFP and FLuc, to measure the *in vivo* survival of the stem cells via Bioluminescence imaging (BLI) and for histological analysis, respectively. After confirming the transduction with FACS, the eGFP/Fluc expressing NSCs will be single cloned before being transduced with a lentiviral (LV) vector carrying the IL-4 gene, for their use in future experiments.

After arrival, the BMSCs, already expressing eGFP and Fluc, were transduced with a LV vector carrying the IL-4 and PURO genes. PURO is included to perform antibiotic selection of only those cells that are successfully transduced. After confirmation of the IL-4 expression in the culture medium with enzyme linked immunosorbent assay (ELISA), the IL-4-producing BMSCs were transplanted in a hemisection SCI mouse model.

The **functional outcome** of the mice treated with BMSC-eGFP-luc-IL-4 was compared with two control groups, those receiving BMSCs only expressing eGFP and Fluc, as well as a PBS-treated group. Lastly, the functional results were correlated with histology, determining the survival of the BMSCs three weeks after transplantation.

This study will reveal whether the use of SCs as carriers of IL-4 can be used as a therapeutic strategy for SCI. A rigorous preclinical evaluation of this combinatorial approach is needed prior to extrapolation to the clinic. New therapeutic strategies for SCI are of major importance, because there is currently no curative therapy and there exists an unmet need for an effective anti-inflammatory treatment for the acute and chronic stages of SCI.

# 2 Materials and methods

## 2.1 Cell cultures

### 2.1.1 BMSCs

The BALB/c-BMSCs, lentivirally transduced with the eGFP and Fluc reporter genes, were kindly provided by Peter Ponsaerts (Laboratory of Experimental Hematology, Vaccine, and Infectious Disease Institute, University of Antwerp). They were cultured in 'BMSC medium' containing: Iscove's Modified Dulbecco's Medium (IMDM) (Invitrogen, Belgium), 10% fetal calf serum (FCS) (FBS Superior, Biochrom AG, Germany), 10% horse serum (HS) (Biochrom AG, Germany) and 1% penicillin/streptomycin (P/S) (5000 units/ml penicillin, 5000 µg/ml streptomycin, Invitrogen, Belgium) in a T25 culture flask. For routine culture, the BMSCs were harvested by trypsin treatment (0,05 %, Invitrogen, Belgium) and were split 1:5 every 7 days. They were incubated at 37°C and 5% $CO_2$.

The provided eGFP/Fluc expressing BMSCs were transferred to a 24-well plate (20 000 cells/well) to grow on poly-L-lysin (PLL) (10 µg/ml, SIGMA, Belgium)-coated glass cover slips, to check the eGFP expression with a Nikon Eclipse 80i fluorescence microscope. For lentiviral transduction with IL-4, they were cultured in a 24-well plate at 10 000 cells/well in 750 µl medium.

### 2.1.2 NSCs

NSCs were cultured from embryonic brains of BALB/c-mice following a protocol adapted from Conti *et al (56)*. Briefly, the embryonic brains (E12-15) were first mechanically dissociated. Next, they were enzymatically dissociated with collagenase A (2 mg/ml, Roche Diagnostics, Belgium), supplemented with DNase I (0,1 mg/ml, Roche, Germany). After two wash steps with Neurobasal-A medium (Invitrogen), the cell population was resuspended and a single cell suspension was obtained by filtering out tissue cubes with a cell strainer (100 µm, BD Biosciences, Belgium). The obtained homogenous cell population was resuspended in 'NSC expansion medium' (NEM), consisting of Neurobasal-A medium (Invitrogen), L-Glutamine (200 mM, Invitrogen), P/S (5000 units/ml penicillin, 5000 µg/ml streptomycin, Invitrogen), human epidermal growth factor (hEGF) (10 ng/ml, ImmunoTools, Germany), human fibroblast growth factor (hFGF-2) (10 ng/ml, ImmunoTools) and N2 supplement (Invitrogen). After a neurosphere population was obtained in a T25 culture flask, an adherently growing NSC-culture was produced by dissociating the neurospheres by accutase treatment (SIGMA, Belgium) and plating the cells out in 10 ml NEM on fibronectin (5 µg/ml in MilliQ, R&D systems, UK)-coated T25 culture flasks. After 24 h, non-adherent cells were removed by changing the NEM. Passage 1 was performed after 7 days. For routine cell culture, the NSCs were detached using accutase treatment when the NSC culture had 90-95% confluence. Cells were harvested by centrifugation (8 min, 300g), after which the pellet was resuspended in 10 ml NEM. Cells were split 1:5 in 10 ml NEM and plated out in new fibronectin-coated T25 flasks. Subculturing was performed every 7 days. The NSC cultures were incubated at 37°C and 5% $CO_2$.

For immunofluorescence staining, harvested NSCs were cultured on fibronectin-coated glass cover slips in a 24-well plate at 25 000 cells per well.

### 2.1.3 *In vitro* differentiation of the NSC culture

To investigate the differentiation potential of the NSCs, they were cultured in 'neural differentiation medium' (NDM). In brief, after accutase treatment, they were replated on PLL (10 µg/ml, SIGMA)-coated glass cover slips in a 24-well plate at a density of 2,5 X $10^4$ cells/well in 750 µl NDM. NDM consists of Neurobasal A medium (Invitrogen), supplemented with L-glutamine (100 mM, Invitrogen) and Neurocult Neural Stem Cell Differentation Supplement (Stem Cell Technologies, France). Every three days the medium was refreshed.

The differentiation potential was investigated by immunofluorescence staining, directly performed on the differentiated NSC cultures.

The effect of IL-4 (Murine IL-4, PeproTech, Inc., UK) on the NSC differentiation was investigated by adding different concentrations of the cytokine (5 ng/ml, 50 ng/ml and 500 ng/ml) to the NDM.

### 2.1.4 Primary neurons

The primary neuron culture was prepared from BALB/c-embryos (E15). Briefly, after removal of the brainstem and the meninges, cerebral cortices were dissociated enzymatically using 2,5% trypsin solution (Invitrogen) in Hank's Buffered Salt Solution (HBSS) (without magnesium and calcium, Invitrogen) for 25 min at 37°C in the water bath. After neutralization of trypsin with 2 ml of FCS, the cortices were treated enzymatically with DNase-I (0,1 mg/ml, Roche). Next, a wash step with 'neuron medium' was followed by resuspension of the cells in the same medium. 'Neuron medium' consists of Neurobasal-A medium (Invitrogen), 1% L-glutamine (200 mM, Invitrogen), 1% P/S (5000 units/ml penicillin, 5000 µg/ml streptomycin, Invitrogen) and 2% B-27 (Invitrogen). The suspension was centrifuged (5 min, 3,00 g, 4°C), the supernatant was harvested and centrifuged again (5 min, 9,00 g, 4°C) to obtain the cells. The pellet was resuspended in 2 ml warm neuron medium.

The cells were used as a positive control for immunofluorescence staining of the differentiated NSCs. The neurons were plated out in a 24-well plate on poly-D-lysine (PDL) (20 µg/ml, SIGMA)-coated cover slips at a density of 150 000 cells/well.

### 2.1.5 Astrocytes

Astrocytes (CCF, Human astrocytoma cell line) were brought into culture in Dulbecco's Modified Eagle's medium-F12 (DMEM/F12) (Invitrogen), supplemented with 10% FCS (FBS Superior, Biochrom AG) and 1% P/S (5000 units/ml penicillin, 5000 µg/ml streptomycin, Invitrogen). For routine culture, the cells were harvested by trypsinisation (0,05%) for 5 min at 37°C. Next, the cell suspension was centrifuged (0,6 g, 5 min, room temperature (RT)). The pellet was resuspended and the cells were split 1:150 in a new T-25 flask.

The astrocytes were used as a positive control for immunofluorescence staining of the differentiated NSCs. For this purpose, the astrocytes were plated on PDL (20 µg/ml, SIGMA)-coated glass cover slips in a 24-well plate at a density of 50 000 cells/well in 500 µl medium.

### 2.1.6 Fibroblasts

The fibroblasts (mouse 3T3-Swiss albino cell line) were grown in DMEM/F12 with Glutamax-I (Invitrogen), supplemented with 10% FCS (FBS Superior, Biochrom AG) and 1% P/S (5000 units/ml penicillin, 5000 µg/ml streptomycin, Invitrogen) in a T25 culture flask.

For routine culturing, medium was removed and the culture was washed with phosphate buffered saline (PBS). Next, cells were detached with trypsin (0,05%) by incubation for 5 min at 37°C. Medium was added to inactivate the trypsin and the cells were harvested by centrifugation (0,72 g, 8 min, RT). The pellet was resuspended and the cell suspension was plated out into a new culture flask at $4x10^4$ cells/flask. Every 3 days the cells were subcultured.

The fibroblast culture was used as a negative control for immunofluorescence staining of the differentiated NSCs. Therefore, the fibroblasts were plated out on glass cover slips in a 24-well plate at a density of 50 000 cells/well.

### 2.1.7 Macrophages

The RAW 264.7 murine cell line (LGC Standards S.a.r.l., Molsheim Cedex, France) was used as a positive control to assess the IL-4 receptor expression on NSCs by real time-PCR and ICC. For subculturing at 70-80% confluency, the cells were mechanically removed from the culture flask surface with a cell scraper. They were split 1:10 in Roswell Park Memorial Institute medium (RPMI) (Invitrogen), supplemented with 10% FCS (FBS Superior, Biochrom AG) and 1% P/S (5000 units/ml penicillin, 5000 µg/ml streptomycin), and incubated at 37°C and 5% $CO_2$.

## 2.2 NSC phenotyping

### 2.2.1 Immunofluorescence staining

First, cells were fixated with 4% paraformaldehyde (PFA) (Merck Eurolab, Belgium) for 20 min. After a washing step with PBS, the cells were permeabilized by incubation in 0,3% Triton (Aldrich, Belgium) during 10 min. Next, Blocking was performed by incubation in a solution of 10% goat serum, 5% Triton and 85% PBS, followed by a washing step with PBS.

Immunofluorescence staining to confirm the stem cell identity of the NSCs was performed using primary antibodies against glial fibrillary acidic protein (GFAP), sex determining region Y-box (SOX2), brain lipid binding protein (BLBP), neuron-specific beta III tubulin (Tuj1) and neuronal nuclei (NeuN) , in combination with Alexa Fluor 568-labeled goat anti-mouse secondary antibody and Alexa Fluor 488-labeled goat anti-rabbit secondary antibody (table 1). The antibodies were diluted in 1% goat serum, 5% Triton and 94% PBS. Briefly, the NSCs were incubated with the primary antibodies (2h, RT). After a washing step, the cells were incubated with the secondary antibodies for 1h at 37°C. As a negative control, NSCs were only incubated with the secondary antibody. Next, the cells were washed and incubated for 10 min at RT with 1% DAPI (4',6-diamidino-2-phenylindole, $3X10^{-7}$ M). Finally, the NSCs were washed with PBS, followed by mounting. Immunofluorescence analysis was performed using a Nikon Eclipse 80i fluorescence microscope. NIS-Elements Viewer 4.0 software was used for image processing.

The same protocol was used for the immunofluorescence staining of the NSCs after differentiation. The same antibodies were used, although double stainings were performed with the anti-GFAP primary antibody in combination with the anti-SOX2, anti-BLBP and anti-Tuj1 primary antibodies. The cell cultures were first incubated with the anti-GFAP primary antibody, followed by incubation with Alexa Fluor 568-labeled goat anti-mouse secondary antibody.

Next, an additional blocking step was performed after which the cell cultures were incubated with the other primary antibodies, followed by incubation with Alexa Fluor 488-labeled goat anti-rabbit secondary antibody. Primary neuron and adult astrocyte cultures were used as positive controls. Fibroblast culture was used as a negative control.

To investigate the effect of the different IL-4 concentrations (5 ng/ml, 50 ng/ml and 500 ng/ml) on the NSC differentiation, ICC using Tuj1/GFAP double staining was performed and the number of astrocytes ($GFAP^+$) and neurons ($Tuj1^+$) in the differentiated NSC cultures was counted using ImageJ software. The total neurite length and the number of branches of the differentiated neurons were also measured with ImageJ software. Per condition, 12 pictures were analyzed.

The presence of the IL-13Rα1 receptor unit on the NSCs was investigated by ICC using antibodies against IL-13Rα1, in combination with Alexa Fluor 488-labeled goat anti-rabbit secondary antibody (table 1). The same protocol as described for the ICC with the neural markers was used, except that the NSCs were not permeabilized with 0,3% Triton because the receptor unit is located on the membrane.

**Table 1: Overview of the primary antibodies with the respective fluorescent labeled secondary antibodies.**

| Antibodies | Working concentration | Vendor/Catalog nr. |
|---|---|---|
| **Primary antibodies** | | |
| Mouse anti-GFAP | 2 µg/ml | Sigma, Belgium, 078K4830 |
| Rabbit anti-SOX2 | 1 µg/ml | Chemicon, Belgium, AB5603 |
| Rabbit anti-BLBP | 2 µg/ml | Chemicon, Belgium, AB9558 |
| Mouse anti-Tuj1 | 8 µg/ml | R&D Systems, UK, MAB1195 |
| Rabbit anti-NeuN | 4 µg/ml | Millipore, Belgium, ABN78 |
| Rabbit anti-IL-13Rα1 | 4 µg/ml | Abcam, UK, Ab79277 |
| **Secondary antibodies** | | |
| Alexa Fluor 568-labeled goat anti-mouse | 4 µg/ml | Invitrogen, Belgium, A11004 |
| Alexa Fluor 488-labeled goat anti-rabbit | 4 µg/ml | Invitrogen, Belgium, A11008 |

GFAP, Glial fibrillary acidic protein; SOX2, Sex determining region Y-box 2; BLBP, Brain lipid binding protein; Tuj1, neuron-specific beta3 tubulin; NeuN, Neuronal nucleus; IL-4Rα, Interleukin-4 receptor alpha; IL-13Rα1, Interleukin-13 receptor alpha 1.

### 2.2.2 Fluorescence activated cell sorting

For phenotyping of the NSC culture, flow cytometric analysis was performed using directly labeled primary antibodies against CD45 and stem cell antigen-1 (Sca-1). Primary antibodies against A2B5 and neural cell adhesion molecule (NCAM) were used in combination with Alexa Fluor 488-labeled goat anti-mouse secondary antibody and Alexa Fluor 488-labeled goat anti-rabbit secondary antibody, respectively (table 2). As negative control unlabelled cells, secondary antibodies alone, and isotype controls for the respective primary antibodies were used (table 2).

Before addition of the primary antibodies, the NSCs ($6x10^4$ cells/well) were washed twice with FACS buffer (PBS-2% FCS). The primary antibodies (1 µg/test) were added to 100 µl of cell suspension in FACS buffer for 45 min at RT in the dark. In the case of secondary antibody staining, cells were washed and incubated with secondary antibodies (1 µg/test) in 100 µl FACS buffer for 30 min at RT in the dark. Next, unlabeled cells were incubated for 10 min at RT in the dark with the live/death stain 7-aminoactinomycin D (7-AAD) (0,25 µg/test, BD Pharmingen, Belgium). Lastly, the cells were washed, resuspended in 200 µl FACS buffer and analyzed with a Becton Dickinson FACSalibur. At least 10 000 cells were analyzed per sample. Flow cytometry data were analyzed using BD CellQuest Pro software.

**Table 2: Overview of the used antibodies and isotype controls.**

| Antibodies | Concentration | Isotype control | Vendor/catalog nr. |
|---|---|---|---|
| **Primary antibodies** | | | |
| PE-labeled rat anti-mouse CD45 | 0,2 mg/ml | PE-labeled IgG2bk Iso Control | BD Biosciences, Belgium, 553081 |
| PE-labeled rat anti-mouse Sca-1 | 0,2 mg/ml | PE/FITC-labeled Simultest γ1/γ2a | eBiosciences, Austria, 12-5981 |
| mouse anti-mouse A2B5 | 1 mg/ml | FITC-labeled IgG1 | Millipore, Belgium, MAB312R |
| Rabbit anti-mouse NCAM | 1 mg/ml | | Chemicon, Belgium, AB5032 |
| **Secondary antibodies** | | | |
| Alexa Fluor 488-labeled goat anti-mouse IgM | 2 mg/ml | | Invitrogen, Belgium, A21042 |
| Alexa Fluor 488-labeled goat anti-rabbit IgM secondary antibody | 2 mg/ml | | Invitrogen, Belgium, A11008 |
| **Isotype controls** | | | |
| PE-labeled IgG2bk Iso Control | 1 mg/ml | | eBiosciences, Austria, 12-4732-42 |
| PE/FITC-labeled Simultest γ1/γ2a | | | Becton Dickinson, Belgium, 342409 |
| FITC-labeled IgG1 | 0,5 mg/ml | | eBiosciences, Austria, 11-5890-81 |

PE, Phycoerythrin; SCA-1, Stem cell antigen-1; NCAM, Neural cell adhesion molecule; Ig, Immunoglobulin; FITC, Fluorescein isothiocyanate.

## 2.3 Analyzing viability of the NSC culture after IL-4 treatment by MTT assay

NSCs were plated into a fibronectin (5 µg/ml in MilliQ, R&D systems)-coated 96-well plate at a density of 100 000 cells per well. After attachment of the NSCs to the plate, the culture medium (NEM supplemented with EGF and bFGF) was replaced by culture medium supplemented with different concentrations of IL-4 (5 ng/ml, 50 ng/ml, 500 ng/ml) (Murine IL-4, PeproTech, Inc.).

After 72 h, the medium was aspirated and replaced by medium supplemented with 10 µl sterile filtered MTT (5 mg/ml, SIGMA) stock solution in PBS, reaching a final concentration of 0,5 mg/ml MTT in each well. After 4h incubation (37°C, 5% CO2), the unreacted dye was aspirated and the insoluble formazan crystals were dissolved in 175 µl of a dimethylsulfoxide (DMSO) – glycine solution. Absorbency was measured at 540-550 nm with the BIO-RAD Benchmark Microplate Reader and Microplate Manager 5.1 software. As blank, culture medium without cells was used.

## 2.4 NSC proliferation assessment after IL-4 treatment by BrdU cell proliferation assay

The BrdU incorporation was performed after treatment of the NSCs (20 000 cells/well) with different concentrations of IL-4 (5 ng/ml, 50 ng/ml, 500 ng/ml) (Murine IL-4, PeproTech, Inc.) for 72h, following the manufacturer's instructions for the BrdU Cell Proliferation Kit (Merck Millipore).

## 2.5 Real time-PCR to analyze IL-4 receptor expression

First, the NSC and RAW 264.7 cultures (positive control) were treated with recombinant IL-4 (72h) (5 ng/ml, Murine IL-4, PeproTech, Inc.) and interferon-γ (IFN-γ) (3h) (10 ng/ml, Murine IFN-γ, PeproTech, Inc.) to assess the effect of the cytokines on the expression of components of the IL-4 receptor. Non-treated cultures were included as control.

Total RNA of the NSCs and RAW 264.7 cultures was purified using the RNeasy Mini Kit (Qiagen, Netherlands), according to the instructions described in the RNeasy Mini Handbook. The purity and the concentration of the isolated RNA were obtained by using the Nanodrop ND1000. Reverse transcription to produce cDNA was performed using the Reverse Transcription System (Promega, USA), according to the instructions of the manufacturer. Real time-PCR was performed using the TaqMan Gene Expression Assay (AB Applied Biosystems, USA), using TaqMan Fast Universal PCR Master Mix, No AmpErase UNG (Life Technologies, Belgium) and IL4ra (Catalog#4331182, Life Technologies), IL13ra1 (Catalog#4453320, Life Technologies), IL13ra2 (Catalog#4331182, Life Technologies) and IL2rg (Catalog#4448892, Life Technologies) primers. B-actin (Catalog#4331182, Life Technologies) and GUS-B (Catalog#4331182, Life Technologies) were used as internal control for normalization.

Amplifications were carried out in a total volume of 20 µl (11 µl PCR reaction mix and 9 µl diluted sample) with the following parameters: polymerase activation at 95°C for 10 min and 40 cycles of PCR; denaturation at 95°C for 15 s and annealing/extension at 60°C for 1 min (StepOnePlus Real-Time PCR System, AB Applied Biosystems). The real time PCR data were processed by StepOne Software v2.2.2 (AB Applied Biosystems). Calculations were performed using the $2^{-\Delta\Delta CT}$ method (57).

The real time-PCR reaction was performed three times. The first time only RNA from untreated RAW 264.7 cells and NSCs RNA was included. Next, all the conditions were included. Per sample, 20 ng cDNA template was used in the real time-PCR reaction mixtures. Lastly, to optimize the real time-PCR, per sample 60 ng cDNA template was included in the reaction mixture. For the IL-4 stimulated NSCs, 28 ng cDNA was included.

The PCR products were separated by agarose gel electrophoresis (1-2 % gel). To the gel a 10 000X dilution of Gel red nucleic acid stain (10 000X in water, Biotium, Belgium) was added to make visualization under UV-light possible. This was done with the Geldoc EQ (Biorad) and Quantity One software. A 100 base pairs (bp) ladder (0,04 µg/µl, Invitrogen) was used as a reference.

## 2.6 Lentiviral vector transduction of BMSCs

eGFP/Fluc-expressing BMSCs were cultured in a 24-well plate at 10 000 cells per well in 750 µl BMSC medium. The next day, the lentiviral vector, carrying the IL-4-gene (10 µl), was added in 300 µl fresh medium. After 24h incubation at 37°C, the BMSC culture was washed and 750 µl fresh medium was added. On the third day after transduction, antibiotic selection with puromycin (1 µg/ml, InvivoGen, France) was started. Next, the cultures were transferred to a 6-well plate, followed by culturing in T-25 flasks.

## 2.7 ELISA to quantify IL-4 expression by the transduced BMSCs

Secretion of IL-4 in the culture medium by the LV transduced BMSCs *in vitro* was determined using the Mouse IL-4 ELISA Ready-SET-Go! kit (eBioscience, Austria), according to the manufacturer's instructions.

## 2.8 Animal experiments

### 2.8.1 BMSC transplantation in the SCI hemisection mouse model

Adult BALB/c-mice (female, 8 to 11 weeks old) (Harlan, the Netherlands) were deeply anesthetized by ketamine (Ketalar, Pfizer, Belgium)-xylazine (Rompun, Bayer, Belgium) (0,012 ml/ gram body weight; ketamine 0,1 mg/ gram body weight and xylazine 0,02 mg/ gram body weight, intraperitoneally i.p.). A laminectomy was performed to expose the dorsal aspect of the spinal cord at T8. Next, a dorsal hemisection was performed with a microscissor to transect the left and right dorsal funiculus, the dorsal horns and the ventral funiculus, resulting in a complete transsection of the dorsomedial and ventral CST (58).

The different experimental groups were treated with IL-4 transduced eGFP/Fluc-BMSCs (11 250 cells in 2,5 µl PBS), eGFP/Fluc-BMSCs (11 000 cells in 2,5 µl PBS) or PBS (2,5 µl) (table 3). The BMSCs or PBS were injected in gel foam patches which were placed on top of the lesion. Next, the muscles were sutured and the skin was closed with wound clips. Analgesic (Temgesic, 6 µg/ml, Reckitt Benckiser Healthcare, Belgium) was injected subcutaneously (150 µl at each side). Glucose was injected intraperitoneally (1 ml). A drop of NaCl (0,9%) on each eye prevented them from drying out. After surgery, the mice were maintained in heated incubators (33°C) until fully awake. After recovery, the mice were returned to their home cages with a close follow up. Bladders were manually voided daily until return of bladder function. The animals were housed in the conventional animal facility of the University of Hasselt, in a temperature-controlled room (20±3°C), on a 12h light/dark schedule, with access to food and water *ad libitum.* The animal experiments were approved by the Ethical Committee of Hasselt University.

**Table 3: Experimental groups**

| Treatment | n |
|---|---|
| PBS | 5 |
| eGFP/Fluc-expressing BMSCs | 4 |
| eGFP/Fluc/IL-4-expressing BMSCs | 5 |

PBS, Phosphate buffered saline; eGFP, enhanced Green Fluorescent Protein; Fluc, Firefly luciferase.

### 2.8.2 Behavioral analysis

**Basso Mouse Scale**

Functional recovery was analyzed by the Basso Mouse Scale (BMS). The BMS measures locomotion, paw placement and trunk stability and exists of 10 scores ranging from 0 (no ankle movement) to 9 (coordinated plantar stepping and normal trunk stability)(59). The mice were scored in an open field during a 4-minute interval by two investigators, who were unaware of the experimental groups. The test was performed every two days from day 1 after injury, during 3 weeks.

**Rotarod**

The Rotarod Performance Test measures general strength. Mice were placed on an accelerating rod (Ugo Basile, Comeris VA, Italy) and latency to fall was recorded in seconds. The time they stayed on was automatically recorded when the mice fell off onto a trigger plate. Before surgery, the mice were trained to stay on the Rotarod for 5 minutes, during three days. After transplantation the test was performed every two days from day 5 after surgery, to avoid additional lesions to the spinal cord. Each trial lasted for a maximum of 5 min. The test was performed for a total of 2 weeks.

### 2.8.3 Analysis of spinal cord tissue sections by histology

Three weeks after transplantaton, mice were anesthesized (60 mg Nembutal/kg bodyweight, intraperitonal i.p.) and transcardially perfused with Ringer solution followed by 4% PFA (Merck Eurolab, Belgium). Spinal cords were dissected and fixed in 5% sucrose in 4% PFA (overnight). Next, the spinal cords were placed in 30% sucrose in 4% PFA (3 days). The spinal cords were embedded in Tissue Tek (O.C.T. Compound, Sakura, Ireland), frozen at -50°C in liquid nitrogen-cooled isopentane (GPR Rectapur, VWR, Belgium) and stored at -80°C. Longitudinal 16-µm-thick cryosections were cut using a Leica CM 3050s/1900 UV cryostat.

Immunohistochemical analysis was performed using primary antibodies against Iba1 (rabbit anti-Iba1, 2 µg/ml, Wako, 019-19741), eGFP (goat anti-eGFP, 1 µg/ml, Abcam, Ab111258) and GFAP (mouse anti-GFAP, 2 µg/ml, Sigma, 078K4830) in combination with Alexa Fluor 555-labeled donkey anti-rabbit secondary antibody (4 µg/ml, Invitrogen, A31572), Alexa Fluor 488-labeled donkey anti-goat (4 µg/ml, Invitrogen, A11055) and Alexa Fluor labeled goat anti-mouse (4 µg/ml, Invitrogen, A11004) secondary antibody, respectively. For these stainings, the same protocol was followed as described for the immunostaining of the NSCs.

Hematoxylin and eosin (HE) staining was performed to investigate the presence of transplanted cells at the lesion site.

## 2.9 Statistical analysis

Statistical analysis was performed with GraphPad Prism Version 5.01. The MTT assay and BrdU assay were analyzed using two-way ANOVA. Real time-PCR results were analyzed using the Kruskal-Wallis test. Data represent mean values ± standard error of the mean (SEM) for the MTT assay and mean values ± standard deviation (SD) for the BrdU assay and the real time-PCR. For *in vitro* cell differentiation studies, results are expressed as mean ± SEM and comparisons were validated using the Mann Whitney test. The locomotion test results are presented as mean values per treatment group ± SEM. Statistical significance was tested by two-way ANOVA. Differences were considered significant with a p-value of <0,05.

# 3 Results

## 3.1 Isolation, culture and *in vitro* characterization of NSCs from BALB/c-mice

In order to obtain NSCs expressing eGFP, Fluc and IL-4, they first had to be isolated, grown and properly characterized *in vitro* having the NSC identity. Next, they can be lentivirally transduced with the desired genes.

Adherently growing NSC cultures were started from embryonic brains of BALB/c-mice. First, neurosphere cultures were initiated from cell suspensions of embryonic brains (figure 3A and B). Secondly, the neurospheres were dissociated by accutase treatment after which adherent NSC-cultures were allowed to grow on fibronectin-coated culture flasks (figure 3C and D). The NSC culture displayed the bipolar morphology (figure 3C) and lattice growth (figure 3D) typical of NSCs.

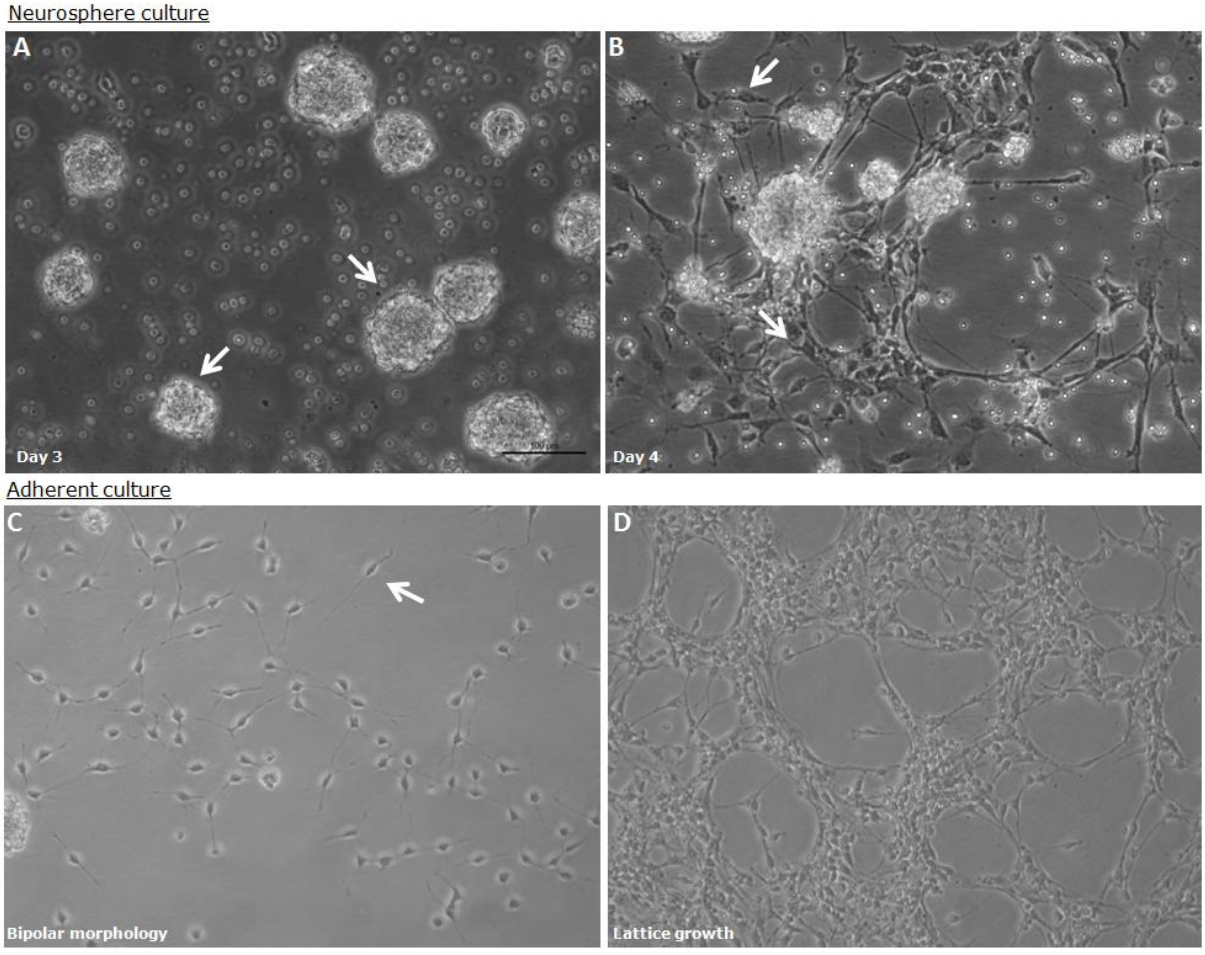


**Figure 3: Culture of NSCs from BALB/c-mice. A)** Representative picture of cultured NSCs growing in neurospheres (white arrows) at day 3 after isolation. **B)** At day 4 after isolation, NSCs (white arrows) started to grow out of the neurospheres. **C and D)** After one week, the neurospheres were dissociated and an adherent NSC-culture was allowed to grow on fibronectin-coated culture flasks (passage 2). In figure C the bipolar morphology (white arrow) of the NSCs is indicated. Figure D shows their typical lattice growth. Pictures were taken with a Nikon eclipse TS100 light microscope. Scale, as indicated in figure A (Scale bar=100 µm).

Besides morphology, the NSCs were characterized *in vitro* by flow cytometry, fluorescence immunocytochemistry and by their differentiation potential.

### 3.1.1 NSCs express A2B5, NCAM, GFAP, BLBP and SOX2, but are negative for CD45, Sca-1, Tuj1 and NeuN

Flow cytometry was used to screen for the presence of specific membrane proteins characteristic for different stem cell types, namely CD45, Sca-1, A2B5 and NCAM. CD45 is a transmembrane glycoprotein specific for hematopoietic stem cells and other cells of hematopoietic origin, and it plays a role in B- and T-cell antigen receptor signal transduction. Sca-1 is a surface marker expressed by hematopoietic stem cells, peripheral B- and T-cells and the myeloid population. A2B5 is a marker specific for the silaogangliosides and sulfatides of the plasma membrane of neurons, endocrine and glial cells. NCAM is a neuronal marker expressed on the surface of neurons from early in development. It holds neurites together during neuron outgrowth and the formation of neuron connections.

Flow cytometric analysis revealed that the cultured populations expressed the neural membrane proteins A2B5 (28,55% positive cells, figure 4A) and NCAM (68,38% positive cells, figure 4B), indicated by cell counts at a higher intensity compared to the controls (purple histograms ↔ open histograms, figure 4A and 4B). Expression of hematopoietic (CD45) or mesenchymal (Sca-1) membrane proteins was not detectable, indicated by the overlap of the purple histogram (specific staining) and the open histogram (control) (figure 4C and 4D).

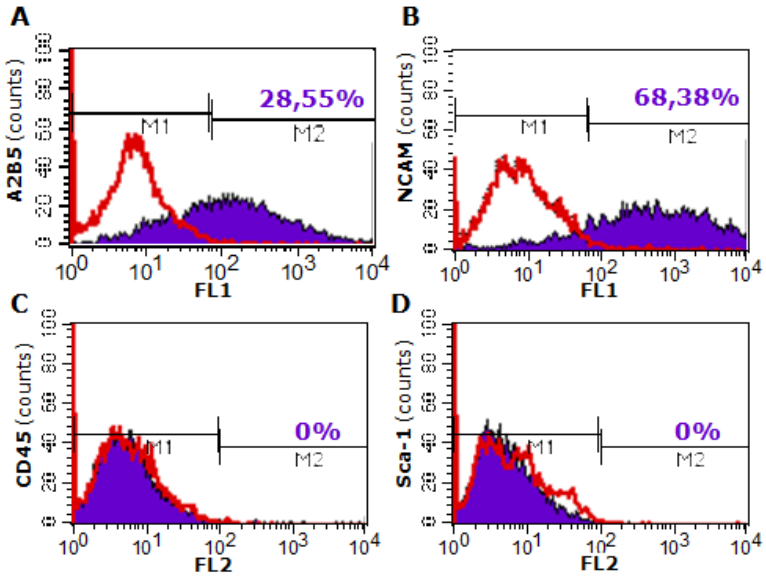


**Figure 4: The NSCs expressed the neural membrane proteins A2B5 and NCAM, but showed no expression of hematopoietic (CD45) or mesenchymal (Sca-1) membrane proteins.** Flow cytometric analysis, indicating the expression pattern of membrane proteins on NSCs (i.e., expression of A2B5 and NCAM, but no expression of CD45 and Sca-1). Open histograms (red line) indicate the controls. Filled histograms (purple) represent the specific stainings. M1 represents the unstained cells, M2 the stained cells. The percentage of positive cells is indicated. The cell counts and the fluorescence intensity are indicated on the x-axis and the y-axis, respectively. The percentage of positive cells was obtained by subtracting the gated percentages of the samples with the gated percentages of the respective isotype controls and the percentage of death cells. When a secondary antibody was used, the gated percentage obtained by using the secondary antibody alone (background) was also subtracted. The percentage of death cells was determined by 7-AAD staining. Representative histograms are shown of three independent flow cytometric analyses, performed at different passages. NCAM, Neural cell adhesion molecule; Sca-1, Stem cell antigen 1.

Besides the determination of the membrane proteins, immunofluorescence staining was also performed to characterize the NSC culture for the expression pattern of intracellular proteins, namely GFAP, BLBP, SOX2, Tuj1 and NeuN. GFAP is a cell specific intermediate filament protein in astrocytes. BLBP is a marker specific for radial glia embryonically and astrocytes postnatally, located in the nucleus or the cytoplasm. The protein is required for the establishment of the radial glial fiber system in the developing brain, moreover for the migration of immature neurons to the established cortical layer. SOX2 is a transcription factor also known as SRY related HMG BOX gene 2 and binds linear DNA, resulting in its bending. This causes the DNA helix to open for some distance. SOX2 is required to maintain self-renewal of undifferentiated embryonic stem cells. Tuj1 is a neuron specific beta III Tubulin neuronal marker. Tubulin is the major constituent of microtubules. Beta III tubulin plays a critical role in proper axon guidance and maintenance. Lastly, NeuN is a DNA-binding, neuron-specific protein.

The NSCs were immunoreactive for GFAP, BLBP and SOX2 (figure 5A-C), but not for Tuj1 and NeuN (figure 5D-E). The negative controls were only incubated with the secondary antibodies. No non-specific binding of these antibodies was visualized (figure S1, Supplementary results).

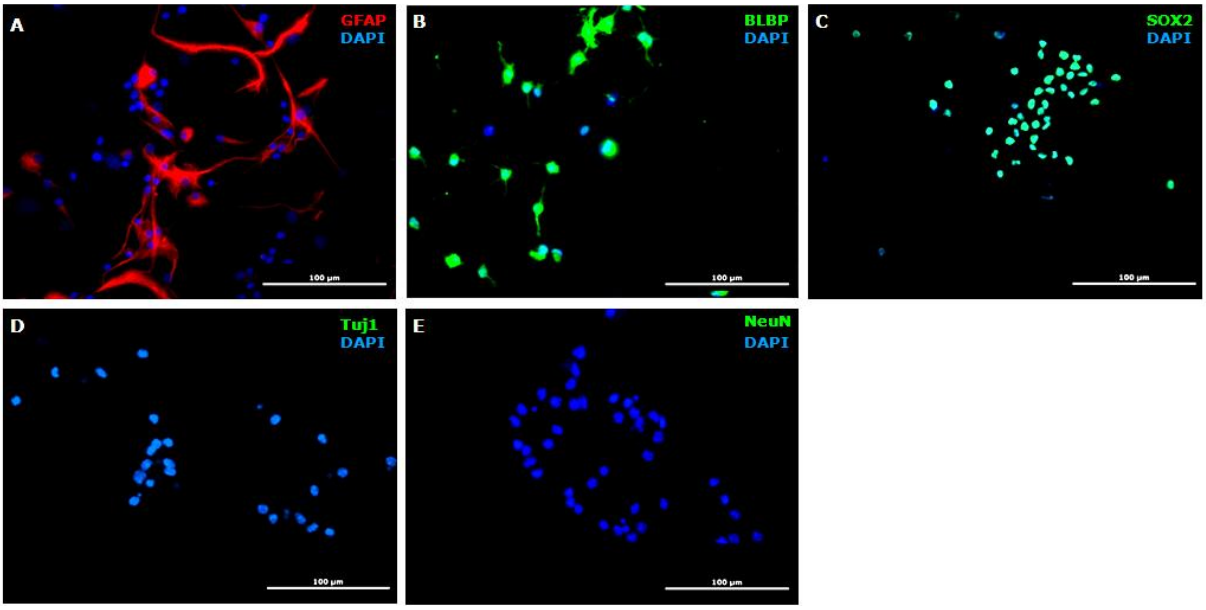


**Figure 5: Characterization of the NSCs from BALB/c-mice by immunofluorescence analysis showed immunoreactivity for GFAP, BLBP and SOX2, but not for Tuj1 and NeuN.** Immunofluorescence staining for GFAP (red), BLBP (green), SOX2 (green), Tuj1 (green) and NeuN (green), counterstained with DAPI (blue). Representative pictures were chosen from three independent immunofluorescence stainings. Pictures were taken using the Nikon Eclipse 80i fluorescence microscope. NIS-Elements Viewer 4.0 software was used for image processing. GFAP, Glial fibrillary acidic protein; BLBP, Brain lipid binding protein; SOX2, Sex determining region Y-box 2; Tuj1, Neuron-specific beta III tubulin; NeuN, Neuronal Nucleus; DAPI, 4',6-diamidino-2-phenylindole. Scale bars: 100 µm, as indicated.

### 3.1.2 **NSCs have the capacity to differentiate into glial and neuronal cell lineages *in vitro***

The NSC identity was further revealed by an *in vitro* differentiation study. After differentiation *in vitro*, the expression pattern of SOX2, BLBP, GFAP and Tuj1 was investigated by immunofluorescence staining. The expression pattern of the proteins on the differentiated NSCs was compared to the expression of the same markers on primary neurons (positive control), astrocytes (positive control) and fibroblasts (negative control). The differentiated NSC-culture showed the morphological presence of astrocytes (figure 6B-Q, white arrows) and neurons (figure 6B-Q, white arrow heads). The differentiated NSCs were immunoreactive for all the tested markers (figure 6E-Q). Negative controls, only incubated with the secondary antibodies, were used to rule out non-specific binding of these antibodies. No signal was present in the negative controls (figure S2, Supplementary results). To control for non-specific binding of the primary antibodies, fibroblasts were used as a negative control. The fibroblasts showed no reactivity for BLBP, GFAP and Tuj1, but were immunoreactive for SOX2 (figure S3, Supplementary results).

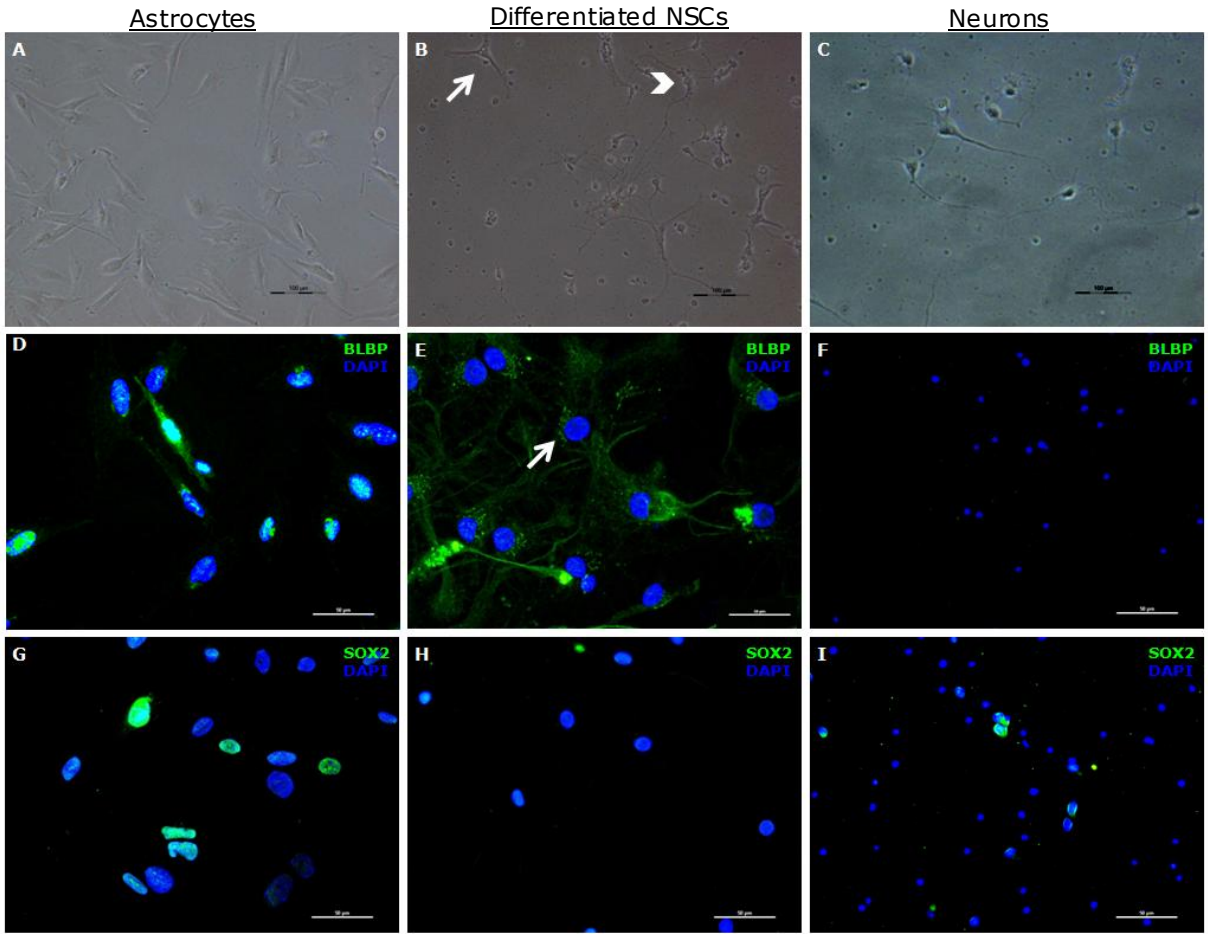

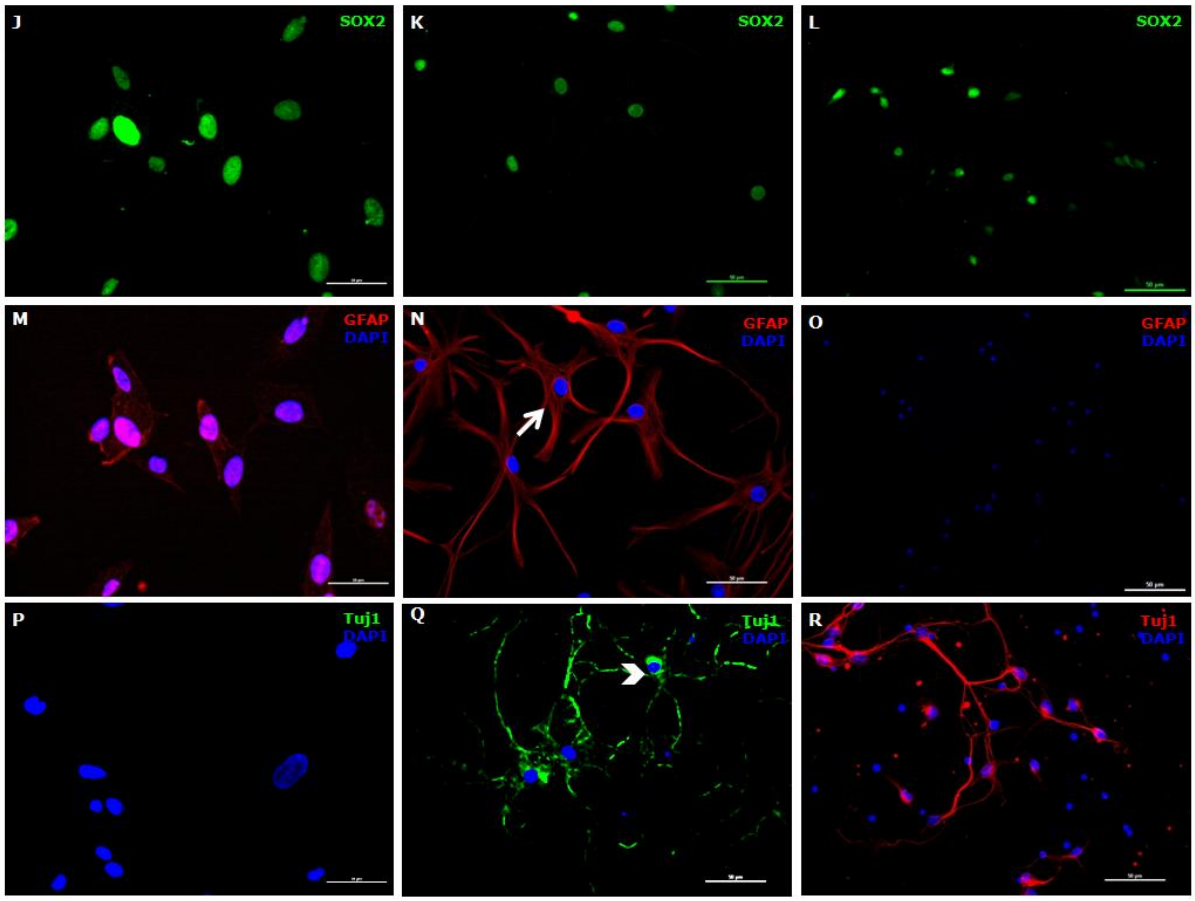


**Figure 6: *In vitro* differentiated NSCs expressed BLBP, SOX2, GFAP and Tuj1, and showed astrocyte and neuron morphology. Column 1**: Immunofluorescence staining of the adult astrocyte culture, used as a positive control. Figure A is a representative bright field microscopy picture of the astrocyte culture. **Column 2**: Immunofluorescence staining of the differentiated NSC-culture. Differentiated astrocytes are indicated by white arrows, differentiated neurons by white arrow heads. Figure B is a representative bright field microscopy picture of the differentiated NSCs. **Column 3**: Immunofluorescence staining of the primary neuron culture, used as a positive control. Figure C is a representative bright field microscopy picture of the primary neuron culture. Immunofluorescence staining was done for BLBP (green), Tuj1 (green in the astrocyte and NSC culture, red in the primary neuron culture), GFAP (red), SOX2 (green) and nucleus (DAPI, blue). The pictures of the SOX2 staining are also included without DAPI-overlay, to show better the presence of the green signal. Light microscopy pictures were taken with a Nikon eclipse TS100 light microscope. Immunofluorescent pictures were taken using the Nikon Eclipse 80i fluorescence microscope. NIS-Elements Viewer 4.0 software was used for image processing. GFAP, Glial fibrillary acidic protein; BLBP, Brain lipid binding protein; SOX2, sex determining region Y-box 2; Tuj1, neuron-specific beta III tubulin; DAPI, 4',6-diamidino-2-phenylindole. Scale bars: 50 and 100 µm, as indicated.

Double stainings were performed combining GFAP with Tuj1, SOX2 and BLBP, to conclude which markers were expressed by the differentiated astrocytes or neurons (figure 7). The differentiated astrocytes were immunoreactive for GFAP (figure 6N and figure 7 A-C), SOX2 (figure 6H-K and figure 7B) and BLBP (figure 6E and figure 7C), but not for Tuj1 (figure 7A), comparable to the adult astrocyte culture (figure 6D-P). Differentiation into neurons was indicated by immunoreactivity for Tuj1 (figure 6N). Double staining showed both the presence of astrocytes ($GFAP^+$) and neurons ($Tuj1^+$) after differentiation in the culture (figure 7A).

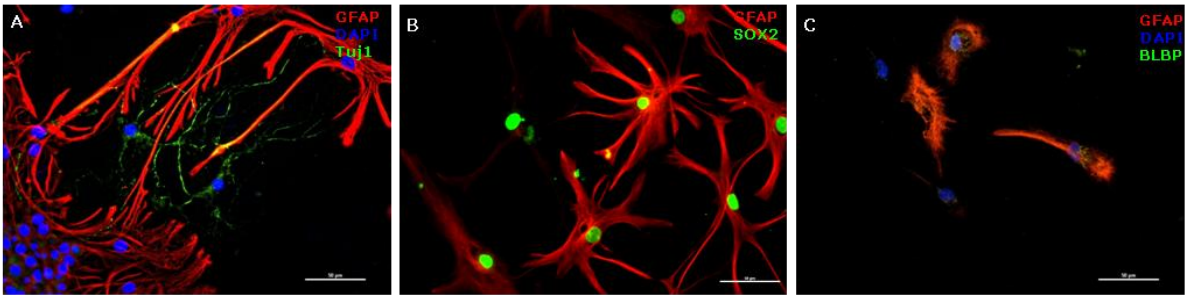


**Figure 7: Immunofluorescence double stainings revealed the presence of both GFAP$^+$ astrocytes and Tuj1$^+$ neurons after *in vitro* differentiation of the NSCs. A)** Immunofluorescence staining of the differentiated NSCs for GFAP (red) and Tuj1 (green), counterstained with DAPI (blue). **B)** Double immunofluorescence staining for GFAP (red) and SOX2 (green). **C)** Double immunofluorescence staining for GFAP (red) and BLBP (green), counterstained with DAPI (blue). Pictures were taken using the Nikon Eclipse 80i fluorescence microscope. NIS-Elements Viewer 4.0 software was used for image processing. GFAP, Glial fibrillary acidic protein; BLBP, Brain lipid binding protein; SOX2, Sex determining region Y-box 2; Tuj1, Neuron-specific beta III tubulin; DAPI, 4',6-diamidino-2-phenylindole. Scale bars: 50 µm, as indicated.

## 3.2 Effect of recombinant mouse IL-4 treatment on the phenotype of NSCs *in vitro*

### 3.2.1 MTT assay indicates no effect on viability of NSCs treated with different concentrations of recombinant mouse IL-4

To investigate the effect of recombinant mouse IL-4 treatment on NSC viability, an MTT assay was performed on NSC-cultures incubated with different concentrations of recombinant mouse IL-4, namely 5 ng/ml, 50 ng/ml and 500 ng/ml. Untreated NSCs were used as control. There was no significant difference between the different groups, although there was a trend suggesting increased viability when the NSC-culture was treated with 5 ng/ml IL-4, compared to the control and the other conditions (figure 8). Passage number (P) did not have a significant effect on the proliferation (figure 8).

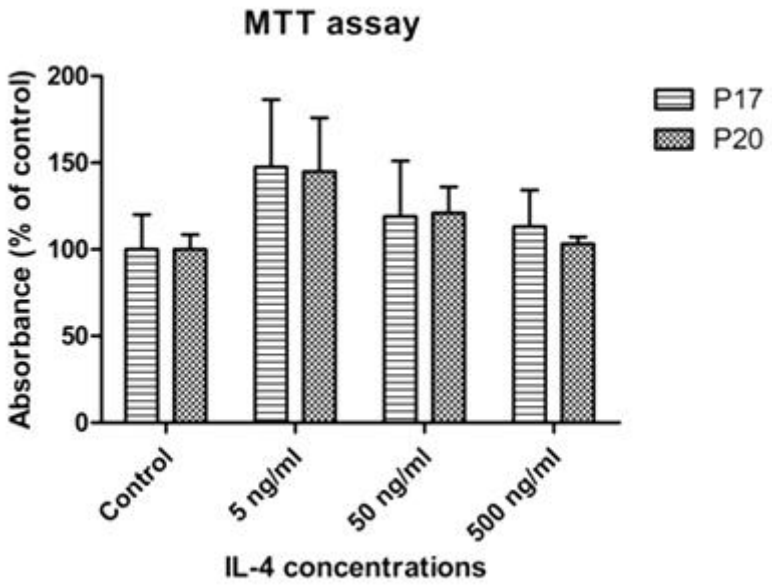

**Figure 8: MTT assay indicated no significant difference in survival after treatment of the NSC-culture with different concentrations of recombinant IL-4.** The NSC-culture (P17 and P20) was treated for 72h with 5 ng/ml, 50 ng/ml and 500 ng/ml mouse recombinant IL-4 in the culture medium (NEM supplemented with EGF and bFGF). Untreated NSCs were used as control. The effects of the IL-4 concentration and the passage on proliferation were not considered significant by two-way ANOVA. The results are presented as mean values normalized to the control ± SEM with n=5 per condition.

### 3.2.2 BrdU cell proliferation assay indicates no effect on proliferation of NSCs treated with different concentrations of recombinant mouse IL-4

A BrdU cell proliferation assay was performed to investigate the effect of different concentrations of IL-4 (5 ng/ml, 50 ng/ml, 500 ng/ml) on proliferation of the NSCs, since BrdU only incorporates in proliferating cells. The different concentrations of IL-4 did not change significantly the proliferation rate, although passage had a significant effect on the results (figure 9). Passage number accounted for a significant difference in proliferation between P12 and P15 in the 5 ng/ml IL-4-treated group (*p<0,05, figure 9) and between P15 and P16 in the 500 ng/ml IL-4-treated group (**p<0,01, figure 9).

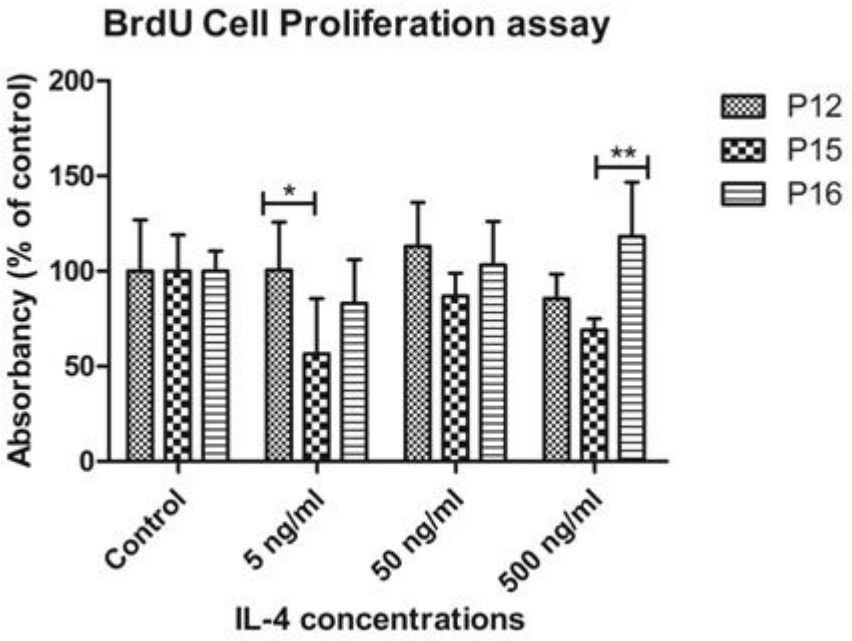


**Figure 9: A BrdU assay indicated no significant difference in cell proliferation after treatment of the NSC culture with different concentrations of IL-4.** The NSC-culture (P12, P15 and P16) was treated for 72h with 5 ng/ml, 50 ng/ml or 500 ng/ml mouse recombinant IL-4 in their culture medium (NEM supplemented with EGF and bFGF). Untreated NSCs were used as control. IL-4 treatment caused no significant difference in proliferation between the different groups, although passage number had a significant effect (P12 vs. P15, 5 ng/ml IL-4 treated group, p<0,05; P15 vs. P16, 500 ng/ml IL-4 treated group, p<0,01). The results are presented as mean values normalized to the control ± SD with n=3 per condition for P12 and n=5 per condition for P15 and P16; *P<0,05 and **P<0,01, as analyzed by two-way ANOVA.

### 3.2.3 Addition of 5 ng/ml IL-4 to differentiating NSCs significantly increases their differentiation into neurons, with additional significant increase in neurite length

To determine the effect of IL-4 on the NSC differentiation potential, a differentiation assay was performed with addition of different IL-4 concentrations (5 ng/ml, 50 ng/ml and 500 ng/ml). After ICC for neuronal (β-III tubulin, Tuj1) and glial markers (GFAP), differentiated neurons and astrocytes were counted. The total neurite length and the number of neurite branches were also determined. Addition of 5 ng/ml IL-4 resulted in a significant increase in neuron differentiation compared to the untreated differentiated NSCs (5 ng/ml treated NSCs vs. untreated NSCs, P=0,0274, figure 10A). The total neurite length also increased significantly after addition of 5 ng/ml (5 ng/ml treated NSCs vs. untreated NSCs, P=0,0233, figure 10B) and 50 ng/ml IL-4 (50 ng/ml treated NSCs vs. untreated NSCs, P= 0,0417, figure 10B). There were no differences in the number of neurite branches between the different conditions, although there was a trend suggesting more neurite branches when 5 ng/ml and 50 ng/ml IL-4 was added to the differentiating NSCs (figure 10C). Addition of IL-4 did not result in differences in astrocyte differentiation (figure 10D).

Representative pictures of the immunofluorescence staining, used to quantify the differentiated neurons/astrocytes, neurite length and sprouting are included. More differentiated neurons are visible in the NSC-culture treated with 5 ng/ml IL-4, compared to the untreated NSCs after differentiation assay (figure 10E). The neurites in the 5 ng/ml and 50 ng/ml IL-4 treated NSC-cultures are visibly longer, compared to the untreated control (figure 10E).

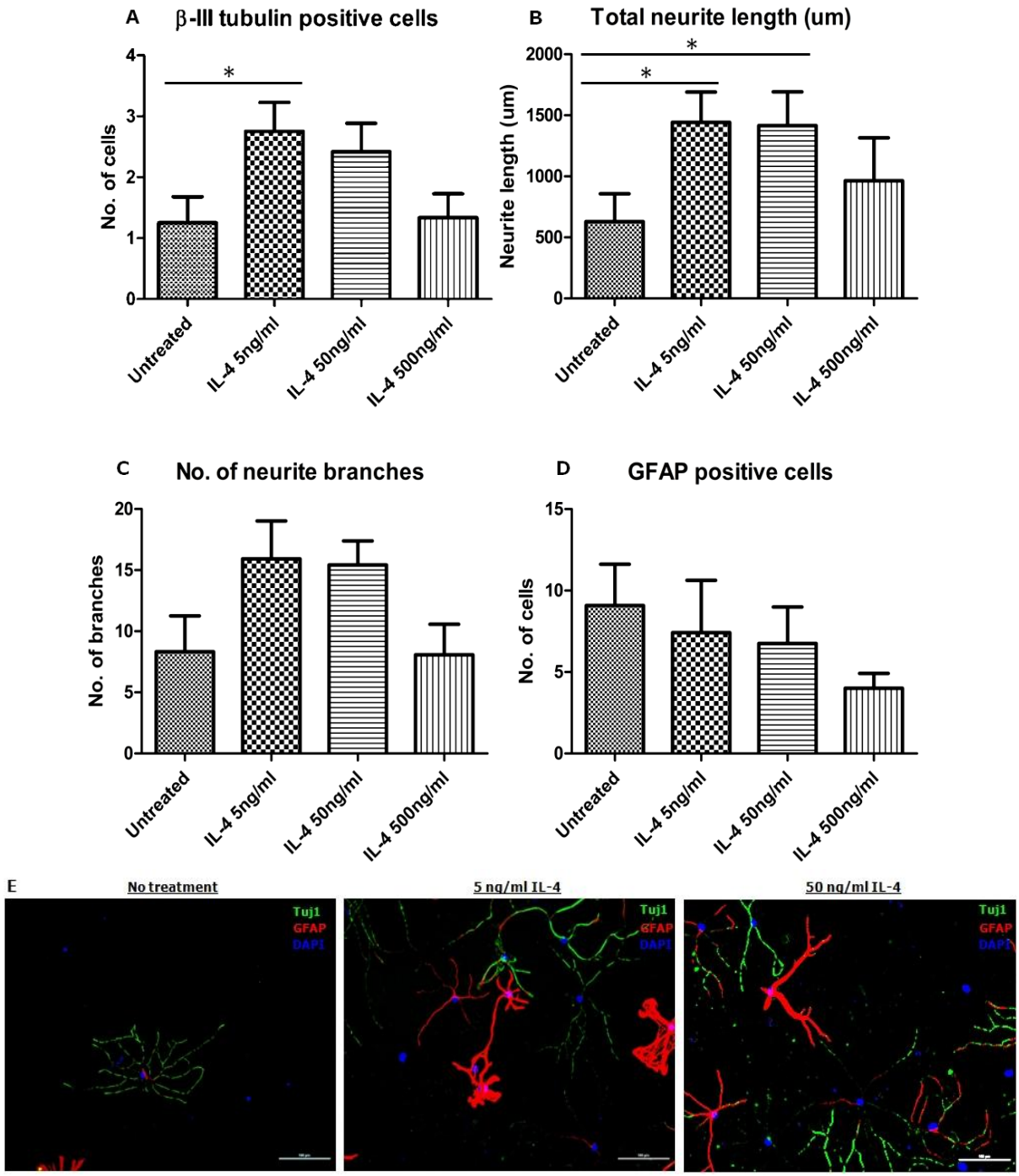


**Figure 10: The number of neurons and the total neurite length increased significantly in the differentiated NSC culture treated with a low dose of IL-4. A)** The number of neurons (β-III tubulin$^+$) increased significantly in the differentiated NSC-culture treated with 5 ng/ml IL-4, compared to the number of neurons in the untreated control (P=0,0274). **B)** The total neurite length increased significantly in the differentiated NSC culture treated with 5 ng/ml IL-4 (P=0,0233) and 50 ng/ml IL-4 (P=0,0417), compared to the total neurite length in the untreated control. **C)** The total number of neurite branches did not change significantly after addition of the different IL-4 concentrations, although there is a trend suggesting more neurite branches in the differentiated NSC-cultures treated with 5 ng/ml IL-4 and 50 ng/ml IL-4, compared to the untreated control. **D)** Addition of IL-4 did not result in differences in astrocyte differentiation. **E)** Representative pictures of the ICC of the differentiated NSC cultures for Tuj1 (green) and GFAP (red) show the presence of more neurons (Tuj1$^+$) in the 5ng/ml IL-4 treated culture then in the untreated control.

The total neurite length is visibly increased in the 5 ng/ml and 50 ng/ml IL-4 treated cultures, compared to the untreated culture. For each condition 12 pictures were used to calculate the quantitative correlates in figures A, B, C and D. Data represent mean values ± SEM; *P<0,05, as analyzed by the Mann-Whitney test. GFAP, Glial fibrillary acidic protein; Tuj1, Neuron-specific beta III tubulin; DAPI, 4',6-diamidino-2-phenylindole; NSC, neural stem cell; IL-4, interleukin-4. Scale bars: 50 µm, as indicated.

## 3.3 IL-4 receptor component expression on NSCs

### 3.3.1 Real-time PCR suggests the expression of IL-13Rα1 on the NSCs after quantitative analysis and expression of IL-13Rα1 and IL-2Rγ after gel electrophoresis, however expression of IL-4Rα is also suggested after IL-4 treatment

Besides the effects of IL-4 on NSCs via modulation of the environment (e.g. via macrophage polarization), an autocrine effect of IL-4 on the stem cells may be observed when they have the IL-4 receptor. Real time-PCR was performed on RNA isolated from the NSCs to reveal the presence of IL-4 receptor components. As a positive control, the murine macrophage cell line RAW264.7 was used. Amplification of the IL-4 receptor components in the macrophage samples showed that the PCR reaction worked (figure 11). The only error reported by the StepOne Software v2.2.2 (AB Applied Biosystems) was a high standard deviation for the expression of the IL-4Rα gene on the untreated RAW 264.7 duplicates (figure 11A). As a negative control, PCR was performed on the reaction mixture without template. This no template control showed no amplification.

Prior to real time-PCR, the NSCs and macrophages were stimulated with IL-4, IL-13 and IFN-γ to determine the effect of these ligands on the receptor unit expression. Addition of IL-4 to the macrophages resulted in a 1,1 fold change in expression of the IL-4Rα unit (figure 11A), a 0,5 fold change in expression in the IL-13Rα1 subunit (figure 11B) and a 1,2 fold change in expression in the IL-2Rγ subunit (figure 11C), compared to the untreated macrophages. Addition of IL-13 resulted in 0,8 fold change in expression of the IL-4Rα gene (figure 11A), 0,6 fold change in expression of the IL-13Rα1 gene (figure 11B) and 1,1 fold change in expression of the IL-2Rγ gene (figure 11C). Addition of IFN-γ increased the expression of the IL-4Rα subunit on the RAW 264.7 cells 3,2 fold (figure 11A). The expression of the IL-13Rα1 gene increased 1,5 fold (figure 11B), but the expression of the IL-2Rγ gene did not increase after addition of IFN-γ (figure 11C).

The real time-PCR results suggested no expression of the IL-4Rα subunit, 1 fold change in expression of the IL-13Rα1 subunit and no expression of the IL-2Rγ subunit on the untreated NSCs (figure 11). Addition of IL-13 to the NSCs did not change the expression of the receptor subunits (Figure 11A, B and C). No conclusion can be formulated about the IFN-γ treated NSCs, because of the high standard deviation (1,8 for the IL-4Rα expression and 3,2 for the IL-13Rα1 expression, figure 11A and B). The IL-4 treated NSCs were excluded from the calculations with the $2^{-\Delta\Delta CT}$ method because a lower cDNA content (28 ng) was used in the PCR reaction, which resulted from a low RNA concentration (18,8 ng/µl) after isolation.

To confirm these qPCR results, the PCR products were separated by length with agarose gel electrophoresis. After amplification of IL-4Rα, IL-13Rα1, IL-13Rα2 and IL-2Rγ, bands are expected at 61, 97, 105 and 65 bp respectively; For the β-actin and Gus-B amplicons, bands are expected at 115 bp and 76 bp.

The untreated as well as the treated RAW 264.7 PCR products show bands at these expected heights (figure 11D). For the untreated NSCs, the 1 fold change in expression of IL-13Rα1 (figure 11B) is confirmed by a band at 97 bp for the receptor unit (figure 11D), although there is also a band present for the IL-2Rγ unit on the gel (65 bp, figure 11D) which is in contrast to the quantitative PCR result (figure 11C). The untreated NSCs showed no dense band, compared to the household genes β-actin (115 bp) and Gus-B (76 bp), for IL-4Rα (61 bp) (figure 11D). The light band present in the lane of this receptor unit may be as a result of non-specific amplification, since a band is also present at this height in the no template control to which no cDNA was added (negative control) (lane 21, gel 2, figure S4 A, Supplementary results). For the NSCs treated with IL-4, bands are visible at the expected heights for all the receptor units and the household genes (figure 11D). For the NSCs treated with IL-13, the quantitative PCR results are confirmed for IL-13Rα1 with a band at 97 bp (figure 11D), but there is also a band present for the IL-2Rγ unit on the gel (65 bp, figure 11D) which is in contrast to the quantitative PCR result (figure 11C). There is again a light band present in the lane of IL-4Rα (61 bp) (figure 11D). The PCR products of the NSCs treated with IFN-γ show bands for IL-4Rα (61 bp), IL-13Rα1 (97 bp) and IL-2Rγ (65 bp) (figure 11D).

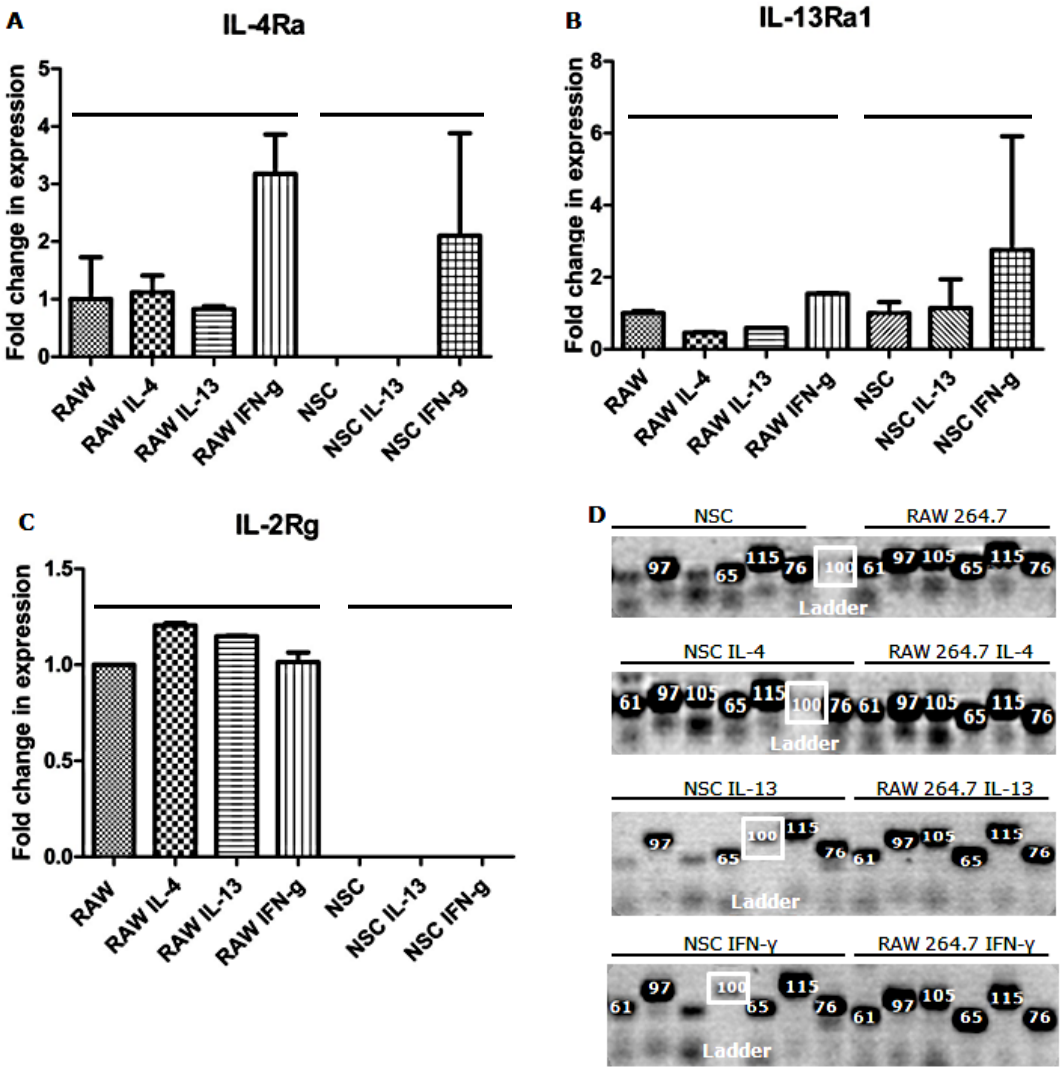

**Figure 11: Real time-PCR suggested the expression of IL-13Rα1 and IL-2Rγ on the NSCs; expression of IL-4Rα was also suggested after IL-4 treatment. A)** Real time-PCR result of IL-4Rα expression on RAW 264.7 cells (positive control) and NSCs; respectively showing untreated, IL-4, IL-13 and IFN-γ treated macrophages, and untreated, IL-13 and IFN-γ treated NSCs. **B)** Real time-PCR result of the IL-13Rα1 expression on RAW 264.7 cells and NSCs. **C)** Real time-PCR result of the IL-2Rγ expression on RAW 264.7 cells and NSCs. The results are presented as mean fold change in expression compared to the untreated cells ± SD (n=2 per condition). The treated macrophage groups were compared with untreated macrophage group and the treated NSC groups with the untreated NSC group, as indicated (black lines). **D)** The electrophoresis result of the PCR products of IL-4Rα (61 bp), IL-13Rα1 (97 bp), IL-13Rα2 (105 bp), IL-2Rγ (65 bp), B-actin (115 bp) and Gus-B (76 bp) is presented for the untreated, IL-4, IL-13 and IFN-γ treated NSCs and RAW 264.7 cells. The 100 bp ladder is indicated by the white box. (*See figure S4, Supplementary results, for a complete image of the gels*). IL-4, interleukin-4; IL-13, interleukin-13; IFN-γ, interferon gamma; NSC, neural stem cell; IL-4Rα, IL-4 receptor alpha; IL-13Rα1, IL-13 receptor alpha 1; IL-13Rα2, IL-13 receptor alpha 2; IL-2Rγ, IL-2 receptor gamma.

### 3.3.2 The NSCs show immunoreactivity for IL-13Rα1

To confirm the results found by qPCR, i.e. IL-13Rα1 expression by the NSCs, ICC with antibodies against IL-13Rα1 was performed. The RAW 264.7 macrophage cell line was again used as a positive control, showing expression of IL-13Rα1 (figure 12A). As a negative control, the cells were only incubated with Alexa Fluor 488 labeled anti-rabbit secondary antibody. This control showed no non-specific binding of the secondary antibody (Figure S5, Supplementary results). The NSCs were immunoreactive for IL-13Rα1 (figure 12B).

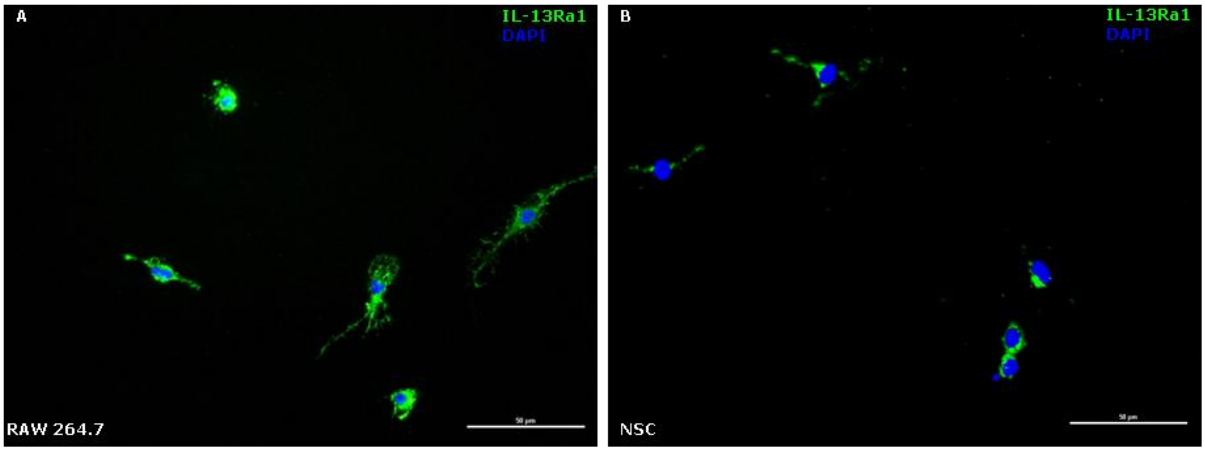


**Figure 12: The NSCs showed immunoreactivity for IL-13Rα1. A)** Immunofluorescence staining of the RAW 264.7 macrophage cell line, used as a positive control, for IL-13Rα1 (green) and nucleus (DAPI, blue). **B)** Immunofluorescence staining of the NSC culture for IL-13Rα1 (green), counterstained with DAPI (blue). Pictures were taken using the Nikon Eclipse 80i fluorescence microscope. NIS-Elements Viewer 4.0 software was used for image processing. IL-13Rα1, IL-13 receptor alpha 1; DAPI, 4',6-diamidino-2-phenylindole; NSC, neural stem cell. Scale bars: 50 µm, as indicated.

## 3.4 Culture and characterization of BALB-c BMSCs expressing eGFP, luciferase and IL-4

To prove the principle of using stem cells as carriers of IL-4 to improve functional outcome, IL-4 producing BMSCs were used. The provided BMSCs already expressed the eGFP and Fluc marker genes, so just their transduction with IL-4 remained.

To check if the provided BMSCs (figure 13A) expressed eGFP, they were cultured in a 24-well plate on coated glass cover slips. After fixation and mounting, they were immediately visualized with the immunofluorescence microscope. A basal expression of eGFP was detectable (figure 13B).

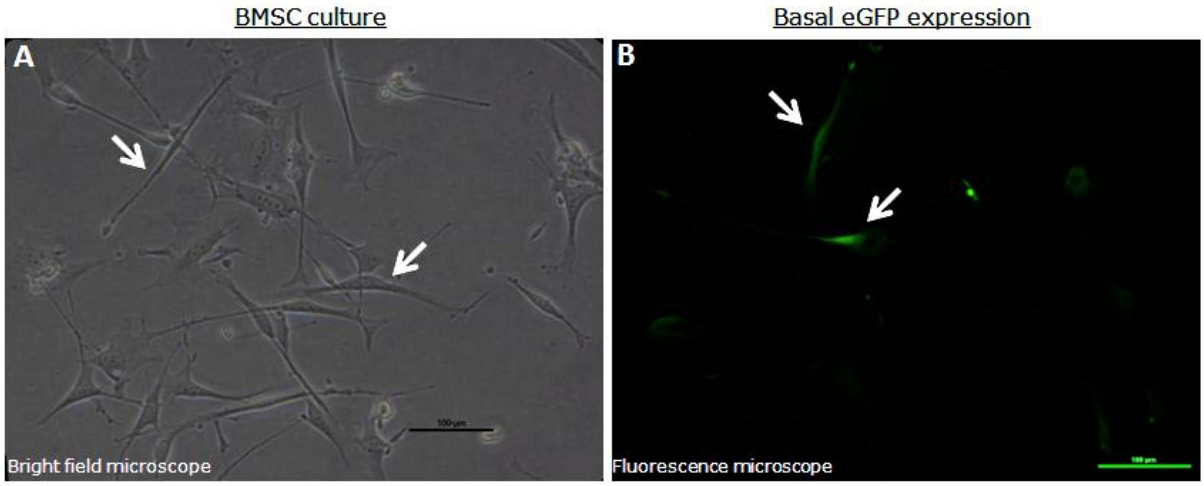


**Figure 13: The BMSC culture expressed eGFP. A)** Representative bright field microscopy picture of cultured BMSCs in a T-25 culture flask (white arrows). **B)** Fluorescence microscope picture showing the basal eGFP expression by the provided BMSCs (white arrows). The bright field microscopy picture was taken with a Nikon eclipse TS100 light microscope. The immunofluorescent picture was taken using the Nikon Eclipse 80i fluorescence microscope. NIS-Elements Viewer 4.0 software was used for image processing. eGFP, enhanced green fluorescent protein. Scale bars: 100 µm, as indicated.

### 3.4.1 The BMSCs secrete IL-4 in the culture medium after transduction

The BMSCs, expressing eGFP and luciferase, were lentivirally transduced with IL-4 in order to transplant these cells in the animal model of SCI. To confirm secretion of the cytokine, the culture medium from the BMSCs transduced with IL-4 was analyzed using ELISA. A serial dilution of the medium was performed, to obtain values fitting the standard curve range: 4 – 500 pg/ml. The 1/10-dilution contained 677,185±27,34 pg/ml IL-4; the 1/100-dilution, 557,348±7,573 pg/ml; the 1/500-dilution, 176,696±22,77 pg/ml; and the 1/1000-dilution 52,293±4,621 pg/ml (figure 14). The IL-4 concentrations of the 1/10- and the 1/100-dilution did not fit in the standard curve range, consequently they were not considered in the calculation of the mean IL-4 concentration. The mean IL-4 concentration secreted in the medium was 703,2065 ng/ml.

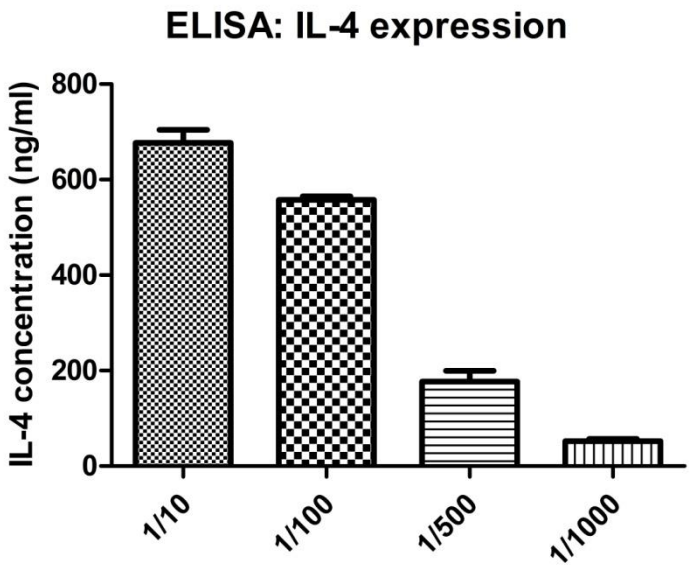


**Figure 14: The BMSCs, lentivirally transduced with IL-4, secreted IL-4 in the culture medium.** The ELISA results are presented as the mean IL-4 concentration (ng/ml) ± SEM of four measurements per condition. The 1/10 diluted medium contained 677,185±27,34 pg/ml IL-4; the 1/100 dilution, 557,348±7,573 pg/ml; the 1/500 dilution, 176,696±22,77 pg/ml; and the 1/1000 dilution, 52,293±4,621 pg/ml. The IL-4 concentrations of the 1/10 and the 1/100 diluted medium did not fit in the standard curve range (4 – 500 pg/ml) and were not considered in the calculation of the mean IL-4 concentration. A representative result is shown of four ELISAs measuring the IL-4 expression in the culture medium at different passages.

## 3.5 Transplantation of IL-4 producing BMSCs after SCI

To determine whether transplantation of IL-4 producing BMSCs improves functional recovery after SCI in mice, two functional tests were performed. The BMS was performed to test locomotion, paw placement and trunk stability and the Rotarod Performance test, to measure general strength. IHC was performed to investigate if the functional test results were reflected by histological findings.

### 3.5.1 Transplantation of IL-4 producing BMSCs does not significantly improve functional outcome after SCI

To investigate if the IL-4-producing BMSCs promote functional recovery, the functional outcome of the treatment group (BMSC-eGFP/Fluc/IL-4) was compared with that of two control groups, namely mice treated with BMSCs expressing only eGFP and Fluc marker genes (BMSC-eGFP/Fluc group) and mice injected with PBS (PBS group). The BMSC-eGFP/Fluc group was included to control the IL-4 effect. The PBS group was included to control the effect of the stem cell transplantation. The BMS revealed no significant differences in locomotion between the different treatment groups (figure 15A). The performance on the Rotarod was also not significantly different between the different treatment groups, which is in line with the BMS result (figure 15B). Together, these results indicated that IL-4 producing BMSC transplantation does not significantly improve functional outcome after SCI.

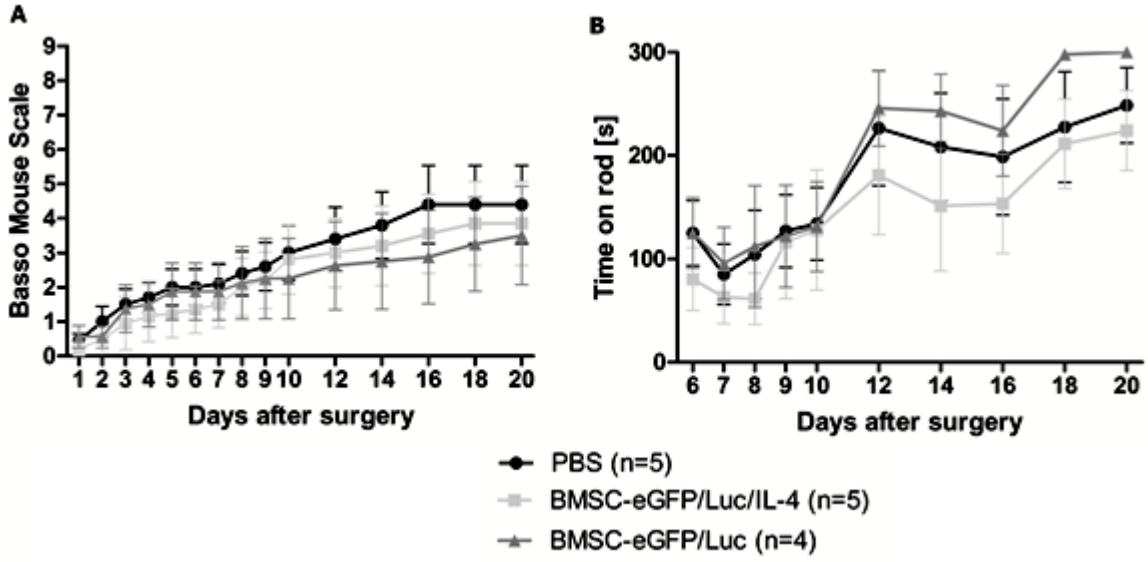


**Figure 15: The BMS and Rotarod test did not reveal significant differences in functional outcome after BMSC-eGFP/Fluc/IL-4 transplantation. A)** The BMS score did not significantly differ between the mice treated with BMSC-eGFP/Fluc/IL-4 and those treated with the BMSCs-eGFP/Fluc or PBS. **B)** The Rotarod test did not show significant differences in the time (s) the mice run on the accelerating rod between the groups. Results are presented as mean values per group ± SEM.

### 3.5.2 Immunofluorescence and histological analysis does not reveal the presence of transplanted BMSCs at the lesion site, three weeks after transplantation

IHC for eGFP (figure 16) and HE staining (*data not shown*) did not reveal the presence of transplanted BMSCs at the lesion site, three weeks after transplantation. Immunofluorescence staining against eGFP and Iba1 on spinal cord tissue sections of animals transplanted with either eGFP/Fluc-BMSCs or eGFP/Fluc/IL-4-BMSCs, showed a cluster of cells ($DAPI^+$) at the lesion site, although it is not clear whether these are BMSCs since the anti-eGFP staining did not show a specific signal compared to the background signal (figure 16A and B).

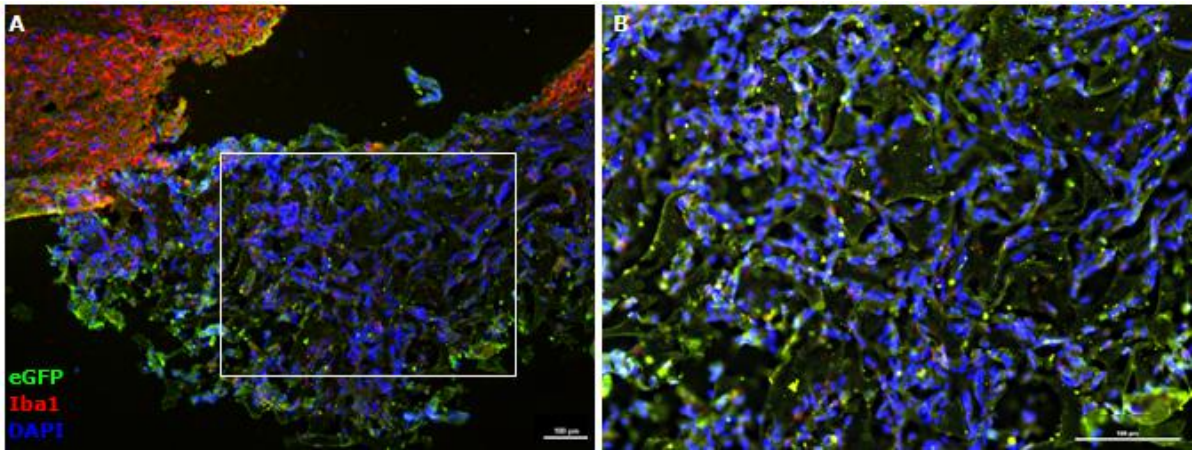


**Figure 16: IHC for eGFP and Iba1 showed a cluster of cells at the lesion site.** IHC for eGFP (green) and Iba1 (red), counterstained with DAPI (nucleus, blue), shows the presence of a cluster of cells at the lesion site. Immunoreactivity against Iba1 (red) indicates the presence of microglia/macrophages. The boxed area in A is shown at a greater magnification (2X) in B.

Representative pictures are shown of three immunostainings per group. The immunofluorescent pictures were taken using the Nikon Eclipse 80i fluorescence microscope. NIS-Elements Viewer 4.0 software was used for image processing. eGFP, enhanced Green Fluorescent Protein; Iba1, Ionized calcium binding adaptor molecule 1; DAPI, 4',6-diamidino-2-phenylindole. Scale bars: 100 µm, as indicated.

However, IHC for Iba1 and GFAP, indicated macrophage/microglia infiltration (figure 16 and figure 17 A-C) and the presence of astrocytes (figure 17 D-F) at the lesion site in all three groups. As a negative control, the spinal cord tissue sections were only incubated with the secondary antibodies, indicating no non-specific binding (figure S6, Supplementary results).

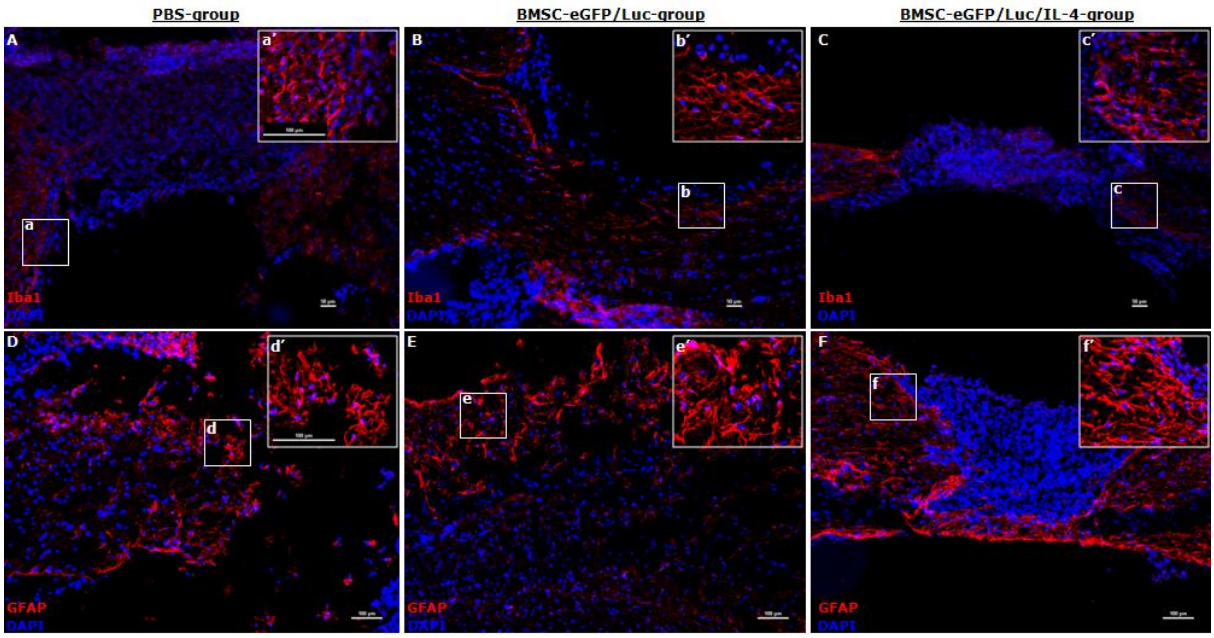


**Figure 17: IHC for Iba-1 and GFAP indicated the presence of microglia/macrophages and astrocytes at the lesion site. A-C)** Immunoreactivity against Iba1 (red) shows the presence of microglia/macrophages in all three groups, as indicated. The nucleus was stained by DAPI (blue). The boxed areas (a, b and c) are shown at a greater magnification (2X) in a', b' and c'. **D-F)** Immunoreactivity against GFAP (red) shows the presence of astrocytes in all three groups, as indicated. The nucleus was stained by DAPI (blue). The boxed areas (d, e and f) are shown at a greater magnification (2X) in d', e' and f'. Representative pictures are shown of three immunostainings per group. The immunofluorescent pictures were taken using the Nikon Eclipse 80i fluorescence microscope. NIS-Elements Viewer 4.0 software was used for image processing. Iba1, Ionized calcium binding adaptor molecule 1; GFAP, Glial fibrillary acidic protein; DAPI, 4',6-diamidino-2-phenylindole. Scale bars: 50 and 100 µm, as indicated. The scale bars in a' and d' measure 100 µm and are representative for b', c', e' and f'.

# 4 Discussion

Currently there is no existing restorative therapy for SCI. Stem cells as carriers of IL-4 could be a promising therapeutic strategy. The aim of this research project was to use IL-4-secreting SCs thereby combining two approaches, namely immunomodulation via IL-4 as well as SC-transplantation. This combination-strategy was chosen because several investigations underscored that stem cell therapy alone is not successful, i.e. temporary regeneration and functional recovery and limited survival and differentiation potential of the stem cells because of the influence of the inflammatory environment after SCI. By using IL-4, we aim to create a more permissive environment, to promote stem cell survival and prolong regeneration.

In the project, BMSCs and NSCs are used as carriers to continuously deliver IL-4 to the site of injury, because transplantation of both stem cell types after SCI was reported to have beneficial effects on regeneration and functional outcome. While characterizing and preparing the NSCs for transplantation, BMSCs were investigated in a pilot study because they were already LV transduced with eGFP and FLuc, and single cloned, when they were provided.

## 4.1 Isolation, culture and *in vitro* characterization of NSCs from BALB/c-mice

In this study, an adherently growing NSC culture was first isolated from embryonic brains of BALB/c-mice. This NSC culture was characterized *in vitro* for the presence of a number of neural markers. Flow cytometric analysis and immunofluorescence staining revealed that the NSCs expressed GFAP, BLBP, SOX2, A2B5 and NCAM. These phenotypical properties are in line with several other reports (31, 56, 60), suggesting a radial glial identity for the NSCs (60). Next, the *in vitro* differentiation potential was investigated to prove multipotency. The NSCs differentiated into astrocytes and neurons, as indicated by their morphology and immunoreactivity for glial and neuronal markers.

Sufficient controls were included to confirm specific binding of the markers. In addition to using a negative control only incubated with the secondary antibody, fibroblasts were used to exclude the possibility of non-specific binding of the primary antibodies. The fibroblasts were negative for BLBP, GFAP and Tuj1, although they were positive for SOX2. This may be explained by the fact that the 3T3 cell line is a mouse embryonic fibroblast cell line and SOX2 is a transcription factor involved in embryonic development and determination of cell fate. It is also involved in pluripotency induction and tumorigenesis. Since the hypertriploid 3T3 cell line is an immortalized cell line, there could be a thin line between them and neoplastic cells. Furthermore, another mouse embryonic fibroblast cell line MEF1 also gave a positive signal for SOX2 (http://www.abcam.com/SOX2-antibody-Embryonic-Stem-Cell-Marker-ab75179.html). Non-specific binding could be further excluded by staining cells certainly not expressing SOX2, like adult microglia.

The differentiated astrocytes showed immunoreactivity for GFAP, SOX2 and BLBP, but not for Tuj1, comparable to the adult astrocyte culture. Although double staining showed the presence of both astrocytes and neurons after differentiation in the culture, a better conclusion about the immunoreactivity of the differentiated neurons to the neuronal and glial markers could be formulated by performing a double staining, using Tuj1 in combination with BLBP, GFAP and SOX2.

The differentiated neurons should be positive for Tuj1 and SOX2, but negative for BLBP and GFAP comparable to the primary neuron culture (31). Furthermore, the tripotential differentiation capacity needs further confirmation by demonstration of the presence of oligodendrocytes after differentiation, for example by testing immunoreactivity for the mouse anti-oligodendrocyte marker O4. However, the differentiation capacity into oligodendrocytes is already demonstrated in several studies upon specific growth factor stimulation (60, 61).

## 4.2 Effect of recombinant mouse IL-4 treatment on the phenotype of neural stem cells *in vitro*

Because the NSCs will be lentivirally transduced with IL-4, the effect of the cytokine on the survival, proliferation and differentiation of the NSCs was tested *in vitro* by MTT assay, BrdU assay and by a differentiation assay conditioned with different concentrations of IL-4 (5, 50, 500 ng/ml).

MTT assay revealed no significant difference between the different groups, although there was a trend suggesting increased viability when the NSC culture was treated with 5 ng/ml IL-4, compared to the control and the other conditions. From the MTT assay it can be concluded that IL-4 is not toxic to the NSCs, since the cell survival was not significantly lower in the IL-4 treated NSCs as compared to the control NSCs. Since MTT is reduced to formazan in the mitochondria of living cells, one cannot conclude from this test whether treatment with IL-4 leads to less cell death or more proliferation. Therefore, a BrdU cell proliferation assay was performed to investigate the effects of the different concentrations of IL-4 on NSC proliferation. Addition of IL-4 to the NSC cultures did not significantly change NSC proliferation, which is in line with the literature since Benedetti *et al* reported no change of the growth rate of NSCs that expressed IL-4 *in vitro* (44). However, subculturing influenced the proliferation significantly. Therefore, future experiments analyzing proliferation should be performed at the same passage of cells. In conclusion, the trend suggested by the MTT assay is probably the result of more surviving NSCs in the culture treated with 5 ng/ml IL-4.

The differentiation assay, followed by ICC for neuronal and glial markers (β-III tubulin and GFAP), showed a significant increase in neuron differentiation when 5 ng/ml IL-4 was added to the NSC-culture as compared to the untreated NSC-culture. The number of astrocytes did not change significantly after addition of the different IL-4 concentrations, although there was a trend suggesting less astrocytic differentiation after IL-4 addition. The increase in neuron differentiation may be in line with the literature because Kiyota *et al* showed that CNS expression of IL-4 can directly enhance neurogenesis, suggesting that IL-4 enhanced neural progenitor cell proliferation and neuronal differentiation (21). Although the astrocytes outnumbered the neurons after differentiation, the neuron/astrocyte ratio increased because of the presence of more neurons and less astrocytes in the culture after differentiation with the lower IL-4 concentrations. Reekmans *et al* also reported more astrocytes (81±4%) then neurons (18±4%) in differentiated NSC-cultures (31). This preference for differentiation toward an astrocytic phenotype could be caused by using EGF in the culture medium, as there is evidence that EGF favors glial differentiation (62).

*In vivo*, transplanted NSCs mainly differentiated into astrocytes, but not into neurons as reported by Reekmans *et al* (31). This may be attributed to the unfavorable microenvironment after SCI. Our aim is to use IL-4 to change the inflammatory spinal cord microenvironment to one more favorable for neuronal differentiation. Supporting our aim, Kiyota *et al* have shown that glial accumulation was partially suppressed by IL-4 treatment in the hippocampal regions of an Alzheimer's disease mouse model (21).

The total neurite length and sprouting were also measured. The total neurite length increased significantly with IL-4 treatment (5 ng/ml and 50 ng/ml), except when the higher IL-4 concentration (500 ng/ml) was added. The number of neurite branches did not change significantly, although there was a trend suggesting increased sprouting compared to the untreated differentiated NSC culture. The neurite outgrowth could be further confirmed by applying different IL-4 concentrations to organotypic brain slices, to determine the effect of IL-4 stimulation on neurite outgrowth in an *in vitro* model closer to the *in vivo* situation (54).

## 4.3 IL-4 receptor subunit expression on NSCs

Besides the indirect effects of IL-4 on stem cell survival and differentiation, via modulation of the immune environment, direct or autocrine effects imply that the stem cells possess the IL-4 receptor. Real time-PCR on RNA isolated from the NSCs was performed to reveal the presence of IL-4 receptor subunits. As a positive control, the murine macrophage cell line RAW264.7 was used. The positive control confirmed that amplification was performed. One error was reported in the data of the positive control, indicating a high standard deviation for the untreated RAW 264.7 cell duplicates. As a negative control, PCR was performed on the reaction mixture without template. This no template-control showed no amplification.

Prior to real time-PCR the NSCs and macrophages were stimulated with IL-4, IL-13 and IFN-γ to determine the effect of these ligands on the receptor unit expression. Addition of IL-4 to the macrophages resulted in a 1,1 fold change in expression of the IL-4Rα unit, a 0,5 fold change in expression in the IL-13Rα1 subunit and a 1,2 fold change in expression in the IL-2Rγ subunit, compared to untreated macrophages. Addition of IL-13 resulted in 0,8 fold change in expression of the IL-4Rα gene, 0,6 fold change in expression of the IL-13Rα gene and 1,1 fold change in expression of the IL-2Rγ gene. However, these results need confirmation. Addition of IFN-γ increased the expression of the IL-4Rα and IL-13Rα1 genes but not of IL-2Rγ, which is in line with the literature. Kota *et al* reported a 4,6 fold change in the expression of the IL-4Rα unit and a 5,7 fold change in the expression of the IL-13rα1 unit, but they reported no changes in the expression of the IL-2Rγ gene after stimulation of RAW 264.7 macrophages with IFN-γ (63).

The real time-PCR results suggested no expression of the IL-4Rα subunit, 1 fold change in expression of the IL-13Rα1 subunit and no expression of the IL-2Rγ subunit on the untreated NSCs. Addition of IL-13 to the NSCs did not change the expression of the receptor subunits. No conclusion can be formulated about the IFN-γ treated NSCs, because of the high standard deviation. The IL-4 treated NSCs were excluded from the calculations with the $2^{-\Delta\Delta CT}$ method because a lower cDNA content was used in the PCR reaction, caused by a low RNA concentration after isolation.

To confirm these results, the PCR products were separated by agarose gel electrophoresis. Bands were visible at the expected heights for all the receptor units (IL-4Rα, IL-13Rα1, IL-13Rα2 and IL-2Rγ) and the household genes (β-actin and GUS-β) after amplification of cDNA of the macrophages, used as a positive control. For the untreated NSCs the quantitative results of the expression of IL-13Rα1 were confirmed by a band on the gel, although there was also a band present for the IL-2Rγ unit which is in contrast to the quantitative PCR result. This could be explained by the fact that a cut-off value of 35 was used for the threshold cycle ($C_T$) values, above which the data were excluded from the calculations. $C_T$ is a relative measure for the concentration of the target in the PCR reaction. $C_T$ values above 35 mean that the concentration of the target in the reaction is very low. For IL-4Rα, the untreated NSCs showed no dense band, compared to the household genes β-actin and Gus-B. The light band present in the lane of this receptor unit could be the result of non-specific amplification or primer dimerization, since a band is also present at this height in the no template control. For the NSCs treated with IL-4, bands are visible at the expected heights for all the receptor units and the household genes. For the NSCs treated with IL-13, the quantitative PCR results are confirmed for IL-13Rα1 with a band on the gel, but again there is also a band present for IL-2Rγ. There is also a light bands present in the lane of IL-4Rα, suggesting non-specific amplification. The PCR products of the NSCs treated with IFN-γ showed bands for IL-4Rα, IL-13Rα1 and IL-2Rγ.

Primer dimerization could be explained by a too low annealing temperature or a too high $MgCl_2$ concentration. There could be many causes of non-specific amplification, like contamination of the cDNA template with genomic DNA (gDNA), contaminated reagents or contamination during reaction set-up. Contamination with gDNA could be controlled by including a no reverse transcriptase control in the real time-PCR set up and by treating the RNA samples with DNAse before reverse transcription. To rule out contamination of the reagents, the real time-PCR should be repeated with newly ordered reagents.

Mutagenesis could also cause bands at unexpected heights. This could be prevented by using Uracil DNA glycosylase, because this enzyme eliminates uracil from DNA molecules by cleaving the N-glycosylic bond and initiating the base-excision repair pathway. Mutagenesis can be controlled by sequencing, followed by alignment with the sequences of the respective murine IL-4 receptor units.

The StepOne Software did not report any amplification in the no template control, although amplicons were visible after agarose gel electrophoresis. A possible explanation for this difference could be that in the instrument settings it was indicated to perform real time-PCR on cDNA template. To amplify RNA and gDNA a different protocol is performed by the StepOnePlus Real-Time PCR System.

All together, the real time-PCR results need further confirmation. The real time-PCR was performed three times, but with different conditions. The first time, only the untreated cells were included. The second time, also cells treated with IL-4, IL-13 and IFN-γ were included. 20 ng cDNA content per sample was used in the PCR reaction mixture. Because of too many errors in the technical replicates and because of amplification errors in the positive control, the real time-PCR was repeated with 60 ng cDNA content per sample in the PCR reaction mixture which lowered the error rate.

However, the PCR needs to be repeated with the same conditions to overcome technical errors like high standard deviations (e.g. pipetting errors), primer dimers and non-specific amplification. To confirm the gene expression changes of the IL-4 receptor units after additions of IL-4, IL-13 and IFN-γ, biological replicates need to be produced by repeating the PCR. To rule out non-specific amplification a negative control, besides the no template control, could be included, like cells with the IL-4/IL-13 receptor genes knocked out (e.g. IL-4Rα $^{-/-}$ lymphocytes) (64).

An additional test to determine the presence of the IL-4 receptor units on the NSCs was carried out by the means of immunofluorescence staining. ICC against IL-13Rα1 revealed its expression by the NSCs. The macrophages, used as a positive control, confirmed specific binding of the primary antibody. Additional, no non-specific binding of the secondary antibody was detected in the negative control.

However, more tests will be necessary to reveal the presence of the IL-4 receptor on the NSCs. Signal transduction through the IL-4 receptor involves three major pathways: Jak-Stat6, Raf-MEK-MAPK and phosphatidylinositol-3'-kinase (PI3K)-Akt (65). The activation of these downstream pathways could be investigated. Lin *et al*, for example, investigated the activation of the IRS/PI3K pathway by IL-4 by immunoprecipitation with anti-IRS-1 and anti-IRS-2 antibodies, after which the immunoprecipitates were subjected to SDS-PAGE and western blot with anti-phosphotyrosine (4G10) antibody (66).

Another possibility is performing a Presence/Absence Experiment, which indicates the presence or absence of a specific nucleic acid sequence (target) in a sample. The actual quantity of target is not determined. The same reagents and reaction set-up as with the qPCR could be used, only the instrument settings are different. The fluorescence data are collected after the PCR is complete, instead of during the amplification like with qPCR. An internal positive control (a short synthetic DNA template) can be used to distinguish between true negative results and reactions affected by PCR inhibitors, incorrect assay setup, or a reagent or instrument failure.

In the literature the presence of the IL-4 receptor on NSCs has not been reported yet, although several reports suggest direct effects of IL-4 on NSCs. Such a reported effect of IL-4 treatment on NSCs is the upregulation of the surface adhesion molecule LFA-1 and the chemokine receptors CXCR4 and CCR5 (24). However, the study did not reveal which pathway, activated by IL-4, lead to this upregulation. Furthermore, Kiyota *et al* showed that CNS expression of IL-4 can directly enhance neurogenesis, likely by enhancing neuronal differentiation and neural progenitor cell proliferation. The mechanisms by which IL-4 induces proliferation may include activation of extracellular signaling-regulated kinases, insulin-response 1 and 2 pathways and the activation of phophatidylinositol-3-kinase and Akt, protecting neurons from apoptosis (21).

The IL-4Rα subunit has been found both in glial cells (67) and in a neuronal cell line (68). In neural-derived cells, the expression of the IL-4 receptor has been reported on a neuroblastoma cell line and on a brain stromal cell line using receptor-ligand binding analysis. However, the presence in glial cells is controversial. One study on the expression of IL-4R mRNA reported that the receptor is expressed on microglia and oligodendrocytes but not on astrocytes. In contrast, Brodie *et al* showed the expression of mRNA levels for IL-4R in glial cells. They argue this may be due to differences in experimental conditions or to the use of different mouse strains (67).

Because neuronal and glial cells have been shown to express IL-4R, it could be suggested that the NSCs (their precursors) express the receptor or will express it in later differentiation stages, but this needs further investigation. Furthermore, cytokines act on cells by inducing the increased expression of several genes. The spectrum of cytokine-induced genes varies depending on the cell type and on the interaction with other cytokines (69).

## 4.4 Culture and characterization of BALB-c BMSCs expressing eGFP, luciferase and IL-4

In this research, IL-4 expressing BMSCs were used to investigate the use of SCs as carriers of IL-4 to improve functional recovery after SCI. With the use of IL-4 producing BMSCs, the effect of tissue replacement by NSCs differentiating to neurons, oligodendrocytes and astrocytes can be ruled out. Only the effect of IL-4 and indirect bystander effects of the BMSCs are investigated.

The BMSCs were already lentivirally transduced with eGFP and Fluc and single cloned, when provided by Peter Ponsaerts' lab. After checking the basal eGFP expression by immunofluorescence microscopy, the BMSCs were transduced with a lentiviral vector carrying IL-4. To confirm secretion of the cytokine, culture medium from BMSCs transduced with IL-4 was analyzed with ELISA. Measuring the IL-4 concentration in the medium at different time points after transduction, showed reduction in IL-4 expression, probably because of a decrease in the growth rate of the BMSCs and because of cell death after transduction. The growth rate of the eGFP/Fluc-transduced BMSCs was slower, compared to the wild type BMSCs. Moreover, after transduction with IL-4, the growth rate further declined. This is in contrast with the literature not reporting phenotypical changes or changes in proliferation after LV transduction (31, 44). These results could be confirmed by a BrdU assay or immunostaining with anti-Ki67-antibodies, comparing proliferation of transduced with non-transduced cells and eGFP/Fluc-expressing cells with IL-4 transduced cells. Cell viability after transduction could be investigated by MTT assay, trypan blue exclusion staining, Hoechst 33342/PI staining or 7-AAD staining.

## 4.5 Transplantation of IL-4 producing BMSCs after SCI

The first goal after transplantation was to investigate if the IL-4-producing BMSCs resulted in functional recovery. This was investigated by performing functional tests, namely the BMS and the Rotarod. The treatment group (IL-4 producing BMSCs) was compared with two control groups, mice treated with BMSCs expressing only eGFP and Fluc marker genes and mice injected with PBS. Because the functional tests did not reveal any significant differences between the treatment group and the control groups, the presence of the BMSCs was investigated by histology to reveal whether the absence of IL-4-producing BMSCs could be an explanation for the functional outcome.

These functional test results were not expected in the light of the reported beneficial effects of IL-4 and BMSC transplantation after SCI. Recently, Payne *et al* showed that gene modified mesenchymal stem cells, overexpressing IL-4, enhanced anti-inflammatory responses and functional recovery in experimental autoimmune demyelination (26). Their results suggested that mesenchymal stem cells as carriers of IL-4 could be a rational approach to promote immunomodulation and tissue protection in a number of degenerative and inflammatory diseases.

Furthermore, our own research group showed that single treatment with recombinant IL-4 significantly promoted functional recovery after SCI. IL-4 improved locomotor restoration from day 1 after operation and histology showed that IL-4 stimulated axon regrowth in the lesioned spinal cord *in vivo* (55), although when IL-4 was delivered 4 days after injury, a decrease in functional outcome was shown by the BMS (*personal communication*).

The test results could be due to absent, low or delayed expression of IL-4, or the absence of BMSCs at the lesion site. Although the transduced BMSCs expressed IL-4 in the culture medium *in vitro*, it could be possible that they did not express IL-4 *in vivo* or that the expression was too low. *In vivo* transgene silencing is frequently reported as a major obstacle. Transgene silencing can result from epigenetic modification of introduced transgenic DNA sequences. This possibility could be investigated, determining the transgene expression, for example, by real time-PCR on mRNA isolated from transplanted spinal cords at different time points after transplantation or by histological assessment (70). Transgene silencing could also result from a reduced cellular activity after transplantation in the spinal cord. Moreover, this reduced cellular activity after transplantation could result in a delayed expression of IL-4, which could cause test results that are in line with the decrease in outcome if a single dose of IL-4 is delivered 4 days after injury as shown by our research group. Therefore, genetic modification needs to result in sufficiently high transgene expression capable of existing even when cellular activity in the spinal cord might be reduced (70).

Per animal 11 000 IL-4 producing BMSCs were transplanted, which correlates with a production of ± 2 ng/ml IL-4 (300 000 cells ≈ 54,2337 ng/ml IL-4). This amount of transplanted cells could be too low to reach a sufficient transgene expression to obtain significant functional improvement. However, more cells were not available by the time of transplantation. Several other research groups transplanted more cells in the order of $1x10^5$ cells (32, 36, 38). Furthermore, because the luciferase gene was included to use BLI to visualize the transplanted stem cells *in vivo*, a minimum of $5x10^4$ cells should be transplanted to obtain a sufficient BLI signal above the background signal (32). In future research, the correct amount of transplanted cells needs to be determined to reach sufficient transgene expression but at a physiological level to avoid toxicity. MTT assay revealed that a concentration of 5 ng/ml IL-4 was not toxic to the NSCs and a trend towards more viability was suggested in comparison with the control and the higher concentrations (50 ng/ml and 500 ng/ml). To determine the effect of the different IL-4 concentrations on the BMSCs, another MTT assay needs to be performed after addition of IL-4 to the BMSC culture.

Another explanation for the absence of significant functional recovery could be immunogenicity of one of the expressed genes, resulting in rejection of the cells. Some authors could not demonstrate a general immunogenic effect of eGFP, while others have shown strong immune response against the protein (71). The immunogenic effect seems to depend on the genetic background of the used mouse strain as an immune response could be elicited in BALB/c mice but not in C57BL/6 mice (71). The Fluc gene could also be immunogenic, as Limberis *et al* reported CD8 T-cell epitopes against Fluc (72). An immune reaction could also be caused by the LV vector. However, the lack of pre-existing immunity to LV vector components may give them a possible advantage over other vector systems derived from viruses that are more widespread (73). The stem cells itself would probably not cause rejection because they are from the same mouse strain.

The gel foam used to locally apply the IL-4 transduced BMSCs to the lesion site could elicit an immune response, although the immunogenicity of gel foam is controversial because some researchers report an immune response (74), while manufacturers claim non-immunogenicity. An example of another transplantation method could be direct injection into the spinal cord with an automatic micro-injector pump with Hamilton Microliter Syringe attached to a stereotactic device to slowly inject the cells. With this method, immune reaction against the gel foam can be excluded and the cells are directly present at lesion site, excluding migration obstruction. The cells could also be administered intravenously but this was reported to have a scarce effectiveness in comparison to intralesional administration (75).

IHC for eGFP, expressed by the transduced BMSCs, and HE staining did not reveal the presence of the transplanted BMSCs at the lesion site, three weeks after transplantation. Immunofluorescence staining of eGFP and Iba1 showed the presence of a cluster of cells ($DAPI^+$) surrounded by macrophages/microglia ($Iba1^+$) at the lesion site, although it is not clear whether these are BMSCs since the anti-eGFP staining did not show a specific signal compared to the background signal. The present cluster could be gel foam including a mixture of BMSCs and SCI-associated inflammatory cells (e.g. lymphocytes) (11), since the gel foam was not removed for tissue processing and the present structure (figure 16B) is similar to the ultrastructural appearance of gel foam under the microscope (76). The absence of a specific signal could be explained by too low or no eGFP expression of the BMSCs *in vivo*, although their *in vitro* expression of eGFP was confirmed. This may be the result of transgene silencing because of epigenetic changes or because of a lower cell activity after transplantation. The amount of transplanted cells could be too low to reach a sufficient transgene expression to obtain detectable eGFP expression, considering this transgene silencing.

The absence of a specific signal for the BMSCs could also be explained by immune reaction against the cells, because of immunogenicity of one of the expressed genes, the vector, the cells themselves, or the gel foam, as explained above. The presence of many $Iba1^+$ cells at the lesion site supports this possibility. Iba1 is a calcium binding protein specifically expressed in microglia and macrophages and is upregulated during the activation of these cells. Microglia become activated upon SCI. They are evident by the first day, increase in number by day 7 and reach a plateau between 2-4 weeks post injury, with reported beneficial and detrimental effects (7). Macrophages are present in the spinal cord from the first week after injury and their activation is maximal between 7-14 days post injury, functioning as phagocytes but also producing pro-inflammatory cytokines and neurotoxins (7). The contribution of these cells to injury or repair is determined by the collective impact of these effects (7). Furthermore, other reports confirm the absence of transplanted SCs 3 weeks after transplantation, because of the pro-inflammatory environment after SCI (31, 38). Bottai *et al* showed that their transplanted NSCs were surrounded by ED1-positive cells (macrophages staining) and later all NSCs were phagocytosed (77). Ide *et al* stated that because BMSCs gradually decrease in number with time in syngeneic and immunosuppressed allogeneic grafts, the BMSCs may not survive long enough to be integrated into the spinal cord tissue (38).

Besides Iba1$^+$ microglia/macrophages, there were also numerous GFAP$^+$ astrocytes present at the lesion site. Together with microglia, astrocytes are the most prevalent cells in the glial scar after SCI. SCI induces the release of glutamate, pro-inflammatory cytokines, ATP, ROS and neurotrophic factors that trigger the activation of glial cells (78). Upon activation, the synthesis of GFAP by astrocytes increases, which is an intermediate filament protein that promotes the synthesis of cytoskeletal supportive structures and modification of the extracellular matrix, contributing to glial scar formation.

All together, a better indication about the viability of the BMSCs could be reached be using BLI at different time points after transplantation (e.g. 1, 2, 7, 14 and 21 days). This imaging method only quantifies living cells since the luciferin-luciferase reaction depends on oxygen and ATP.

In conclusion, future studies are needed to investigate and to optimize the IL-4 expression by transduced SCs *in vivo,* to reveal their therapeutic potential for the local delivery of anti-inflammatory cytokines to improve recovery after SCI.

# 5 Conclusion

The goal of the present project was the transplantation of SCs as carriers of IL-4 to improve functional outcome after SCI. NSCs and BMSCs were used, because both previously showed promising effects after transplantation in SCI. Therefore, first the NSCs were characterized, after which they can be transduced and single cloned to become IL-4 producing NSCs for their use in future experiments. Although their differentiation into oligodendrocytes needs to be confirmed, the differentiation to neuronal and glial lineages is already a good indication of the differentiation potential as oligodendrocytes are themselves derived from glial lineages. Addition of different concentrations of IL-4 to the NSC culture revealed no significant differences in viability and proliferation, which is a promising result for their use *in vivo* as the transduced NSCs will secrete IL-4 in their own microenvironment. The effect of IL-4 on the differentiation potential of the NSCs is also promising, resulting in a significant increase in neuron differentiation and the total neurite length when low concentrations of IL-4 were applied, compared to the untreated NSCs. In further experiments the *in vivo* effect of IL-4 on neuronal differentiation and survival needs to be investigated. However, besides neuronal differentiation, beneficial effects of IL-4 on functional outcome could by caused by axon regeneration, prolongation of NSC survival, immunomodulation and other bystander effects.

In the literature, direct (autocrine) and indirect effects of IL-4 on NSCs are suggested. The real time-PCR and ICC results suggested the presence of the IL-4 receptor component IL-13Rα1 on the NSCs, but this needs further confirmation. An autocrine effect could result in excessive proliferation of the NSCs or toxicity, when IL-4 is overexpressed. However, our *in vitro* test results of the effect of IL-4 on the survival and the proliferation do not point towards such a possibility. The *in vivo* concentration of IL-4 produced by the IL-4 transduced NSCs needs to be investigated and it needs to be confirmed that this is a physiological concentration not causing toxicity or excessive proliferation, considering an autocrine effect.

In the second part of the project, a pilot study with IL-4 producing BMSCs was performed to investigate whether the use of stem cells is a good way to deliver IL-4 to the site of injury, continuously, at a low concentration. Functional tests did not indicate a significant difference in recovery between the animals transplanted with IL-4 transduced BMSCs and the control groups. This was probably due to absent, low or delayed expression of IL-4, or the absence of the BMSCs at the lesion site after transplantation. The former could be caused by transgene silencing due to epigenetic changes or a lower cell activity after transplantation, the latter by immunogenicity resulting in rejection of the cells. Furthermore, the amount of transplanted BMSCs could be too low to obtain sufficiently high transgene expression. Therefore, the correct amount of transplanted cells needs to be determined to reach sufficient transgene expression, but at a physiological level to avoid toxicity. Although IL-4 producing BMSCs were used to test their regenerative potential, NSCs are preferred above BMSCs because they may possess intrinsic properties that are superior to BMSCs to aim for CNS regeneration with stem cell therapy.

In further research, IL-4 producing NSCs will be used to investigate whether their immunomodulatory and regenerative functions promote axon regeneration, neuronal differentiation and NSC-survival to improve functional recovery after transplantation in SCI.

# References


1. Thuret S, Moon LD, Gage FH. Therapeutic interventions after spinal cord injury. Nature reviews Neuroscience. 2006;7(8):628-43. Epub 2006/07/22.
2. Harel NY, Strittmatter SM. Can regenerating axons recapitulate developmental guidance during recovery from spinal cord injury? Nature reviews Neuroscience. 2006;7(8):603-16. Epub 2006/07/22.
3. Schwab JM, Brechtel K, Mueller CA, Failli V, Kaps HP, Tuli SK, et al. Experimental strategies to promote spinal cord regeneration--an integrative perspective. Progress in neurobiology. 2006;78(2):91-116. Epub 2006/02/21.
4. Ronsyn MW, Berneman ZN, Van Tendeloo VF, Jorens PG, Ponsaerts P. Can cell therapy heal a spinal cord injury? Spinal cord. 2008;46(8):532-9. Epub 2008/03/19.
5. McDonald JW, Sadowsky C. Spinal-cord injury. Lancet. 2002;359(9304):417-25. Epub 2002/02/15.
6. Weil ZM, Norman GJ, DeVries AC, Nelson RJ. The injured nervous system: a Darwinian perspective. Progress in neurobiology. 2008;86(1):48-59. Epub 2008/07/08.
7. Trivedi A, Olivas AD, Noble-Haeusslein LJ. Inflammation and Spinal Cord Injury: Infiltrating Leukocytes as Determinants of Injury and Repair Processes. Clinical neuroscience research. 2006;6(5):283-92. Epub 2007/12/07.
8. Fitch MT, Silver J. CNS injury, glial scars, and inflammation: Inhibitory extracellular matrices and regeneration failure. Experimental neurology. 2008;209(2):294-301. Epub 2007/07/10.
9. Teng YD, Lavik EB, Qu X, Park KI, Ourednik J, Zurakowski D, et al. Functional recovery following traumatic spinal cord injury mediated by a unique polymer scaffold seeded with neural stem cells. Proceedings of the National Academy of Sciences of the United States of America. 2002;99(5):3024-9. Epub 2002/02/28.
10. Okano H, Ogawa Y, Nakamura M, Kaneko S, Iwanami A, Toyama Y. Transplantation of neural stem cells into the spinal cord after injury. Seminars in cell & developmental biology. 2003;14(3):191-8. Epub 2003/09/02.
11. Donnelly DJ, Popovich PG. Inflammation and its role in neuroprotection, axonal regeneration and functional recovery after spinal cord injury. Experimental neurology. 2008;209(2):378-88. Epub 2007/07/31.
12. Russo I, Barlati S, Bosetti F. Effects of neuroinflammation on the regenerative capacity of brain stem cells. Journal of neurochemistry. 2011;116(6):947-56. Epub 2011/01/05.
13. Ruff CA, Wilcox JT, Fehlings MG. Cell-based transplantation strategies to promote plasticity following spinal cord injury. Experimental neurology. 2011. Epub 2011/02/22.
14. Tetzlaff W, Okon EB, Karimi-Abdolrezaee S, Hill CE, Sparling JS, Plemel JR, et al. A systematic review of cellular transplantation therapies for spinal cord injury. Journal of neurotrauma. 2011;28(8):1611-82. Epub 2010/02/12.
15. Soria JA, Arroyo DS, Gaviglio EA, Rodriguez-Galan MC, Wang JM, Iribarren P. Interleukin 4 induces the apoptosis of mouse microglial cells by a caspase-dependent mechanism. Neurobiology of disease. 2011;43(3):616-24. Epub 2011/06/01.
16. Chatila TA. Interleukin-4 receptor signaling pathways in asthma pathogenesis. Trends in molecular medicine. 2004;10(10):493-9. Epub 2004/10/07.
17. Lee SI, Jeong SR, Kang YM, Han DH, Jin BK, Namgung U, et al. Endogenous expression of interleukin-4 regulates macrophage activation and confines cavity formation after traumatic spinal cord injury. Journal of neuroscience research. 2010;88(11):2409-19. Epub 2010/07/14.
18. Kigerl KA, Gensel JC, Ankeny DP, Alexander JK, Donnelly DJ, Popovich PG. Identification of two distinct macrophage subsets with divergent effects causing either neurotoxicity or regeneration in the injured mouse spinal cord. The Journal of neuroscience : the official journal of the Society for Neuroscience. 2009;29(43):13435-44. Epub 2009/10/30.
19. Kuo HS, Tsai MJ, Huang MC, Chiu CW, Tsai CY, Lee MJ, et al. Acid fibroblast growth factor and peripheral nerve grafts regulate Th2 cytokine expression, macrophage activation, polyamine

synthesis, and neurotrophin expression in transected rat spinal cords. The Journal of neuroscience : the official journal of the Society for Neuroscience. 2011;31(11):4137-47. Epub 2011/03/18.
20. Hendrix S, Nitsch R. The role of T helper cells in neuroprotection and regeneration. J Neuroimmunol. 2007;184(1-2):100-12. Epub 2007/01/03.
21. Kiyota T, Okuyama S, Swan RJ, Jacobsen MT, Gendelman HE, Ikezu T. CNS expression of anti-inflammatory cytokine interleukin-4 attenuates Alzheimer's disease-like pathogenesis in APP+PS1 bigenic mice. FASEB journal : official publication of the Federation of American Societies for Experimental Biology. 2010;24(8):3093-102. Epub 2010/04/08.
22. Derecki NC, Cardani AN, Yang CH, Quinnies KM, Crihfield A, Lynch KR, et al. Regulation of learning and memory by meningeal immunity: a key role for IL-4. The Journal of experimental medicine. 2010;207(5):1067-80. Epub 2010/05/05.
23. Koeberle PD, Gauldie J, Ball AK. Effects of adenoviral-mediated gene transfer of interleukin-10, interleukin-4, and transforming growth factor-beta on the survival of axotomized retinal ganglion cells. Neuroscience. 2004;125(4):903-20. Epub 2004/05/04.
24. Guan Y, Jiang Z, Ciric B, Rostami AM, Zhang GX. Upregulation of chemokine receptor expression by IL-10/IL-4 in adult neural stem cells. Experimental and molecular pathology. 2008;85(3):232-6. Epub 2008/09/09.
25. Lowenthal JW, Castle BE, Christiansen J, Schreurs J, Rennick D, Arai N, et al. Expression of high affinity receptors for murine interleukin 4 (BSF-1) on hemopoietic and nonhemopoietic cells. J Immunol. 1988;140(2):456-64. Epub 1988/01/15.
26. Payne N, Dantanarayana A, Sun G, Moussa L, Caine S, McDonald C, et al. Early intervention with gene-modified mesenchymal stem cells overexpressing interleukin-4 enhances anti-inflammatory responses and functional recovery in experimental autoimmune demyelination. Cell adhesion & migration. 2012;6(3). Epub 2012/05/10.
27. He S, Nakada D, Morrison SJ. Mechanisms of stem cell self-renewal. Annual review of cell and developmental biology. 2009;25:377-406. Epub 2009/07/07.
28. Potten CS, Loeffler M. Stem cells: attributes, cycles, spirals, pitfalls and uncertainties. Lessons for and from the crypt. Development. 1990;110(4):1001-20. Epub 1990/12/01.
29. Blau HM, Brazelton TR, Weimann JM. The evolving concept of a stem cell: entity or function? Cell. 2001;105(7):829-41. Epub 2001/07/06.
30. Muller FJ, Snyder EY, Loring JF. Gene therapy: can neural stem cells deliver? Nature reviews Neuroscience. 2006;7(1):75-84. Epub 2005/12/24.
31. Reekmans KP, Praet J, De Vocht N, Tambuyzer BR, Bergwerf I, Daans J, et al. Clinical potential of intravenous neural stem cell delivery for treatment of neuroinflammatory disease in mice? Cell transplantation. 2011;20(6):851-69. Epub 2010/11/26.
32. Bergwerf I, De Vocht N, Tambuyzer B, Verschueren J, Reekmans K, Daans J, et al. Reporter gene-expressing bone marrow-derived stromal cells are immune-tolerated following implantation in the central nervous system of syngeneic immunocompetent mice. BMC biotechnology. 2009;9:1. Epub 2009/01/09.
33. Peister A, Mellad JA, Larson BL, Hall BM, Gibson LF, Prockop DJ. Adult stem cells from bone marrow (MSCs) isolated from different strains of inbred mice vary in surface epitopes, rates of proliferation, and differentiation potential. Blood. 2004;103(5):1662-8. Epub 2003/11/01.
34. Chamberlain G, Fox J, Ashton B, Middleton J. Concise review: mesenchymal stem cells: their phenotype, differentiation capacity, immunological features, and potential for homing. Stem Cells. 2007;25(11):2739-49. Epub 2007/07/28.
35. Dominici M, Le Blanc K, Mueller I, Slaper-Cortenbach I, Marini F, Krause D, et al. Minimal criteria for defining multipotent mesenchymal stromal cells. The International Society for Cellular Therapy position statement. Cytotherapy. 2006;8(4):315-7. Epub 2006/08/23.
36. Lu P, Jones LL, Tuszynski MH. BDNF-expressing marrow stromal cells support extensive axonal growth at sites of spinal cord injury. Experimental neurology. 2005;191(2):344-60. Epub 2005/01/15.

37. Philippe B. Culture and use of mesenchymal stromal cells in phase I and II clinical trials. Stem Cells International. 2010

2010:1-8.
38. Ide C, Nakai Y, Nakano N, Seo TB, Yamada Y, Endo K, et al. Bone marrow stromal cell transplantation for treatment of sub-acute spinal cord injury in the rat. Brain research. 2010;1332:32-47. Epub 2010/03/24.
39. Wright KT, El Masri W, Osman A, Chowdhury J, Johnson WE. Concise review: Bone marrow for the treatment of spinal cord injury: mechanisms and clinical applications. Stem Cells. 2011;29(2):169-78. Epub 2011/07/07.
40. Nakajima H, Uchida K, Rodriguez Guerrero A, Watanabe S, Sugita D, Takeura N, et al. Transplantation of Mesenchymal Stem Cells Promotes the Alternative Pathway of Macrophage Activation and Functional Recovery after Spinal Cord Injury. Journal of neurotrauma. 2012. Epub 2012/01/12.
41. Phinney DG, Prockop DJ. Concise review: mesenchymal stem/multipotent stromal cells: the state of transdifferentiation and modes of tissue repair--current views. Stem Cells. 2007;25(11):2896-902. Epub 2007/09/29.
42. Rebelatto CK, Aguiar AM, Moretao MP, Senegaglia AC, Hansen P, Barchiki F, et al. Dissimilar differentiation of mesenchymal stem cells from bone marrow, umbilical cord blood, and adipose tissue. Exp Biol Med (Maywood). 2008;233(7):901-13. Epub 2008/05/01.
43. Tropel P, Noel D, Platet N, Legrand P, Benabid AL, Berger F. Isolation and characterisation of mesenchymal stem cells from adult mouse bone marrow. Experimental cell research. 2004;295(2):395-406. Epub 2004/04/20.
44. Benedetti S, Pirola B, Pollo B, Magrassi L, Bruzzone MG, Rigamonti D, et al. Gene therapy of experimental brain tumors using neural progenitor cells. Nature medicine. 2000;6(4):447-50. Epub 2000/03/31.
45. Choi JJ, Yoo SA, Park SJ, Kang YJ, Kim WU, Oh IH, et al. Mesenchymal stem cells overexpressing interleukin-10 attenuate collagen-induced arthritis in mice. Clinical and experimental immunology. 2008;153(2):269-76. Epub 2008/08/21.
46. Hu W, Wang J, He X, Zhang H, Yu F, Jiang L, et al. Human umbilical blood mononudear cell-derived mesenchymal stem cells serve as interleukin-21 gene delivery vehicles for epithelial ovarian cancer therapy in nude mice. Biotechnology and applied biochemistry. 2011;58(6):397-404. Epub 2011/12/17.
47. Ryu CH, Park SH, Park SA, Kim SM, Lim JY, Jeong CH, et al. Gene therapy of intracranial glioma using interleukin 12-secreting human umbilical cord blood-derived mesenchymal stem cells. Human gene therapy. 2011;22(6):733-43. Epub 2011/01/26.
48. Seo SH, Kim KS, Park SH, Suh YS, Kim SJ, Jeun SS, et al. The effects of mesenchymal stem cells injected via different routes on modified IL-12-mediated antitumor activity. Gene therapy. 2011;18(5):488-95. Epub 2011/01/14.
49. Xu G, Jiang XD, Xu Y, Zhang J, Huang FH, Chen ZZ, et al. Adenoviral-mediated interleukin-18 expression in mesenchymal stem cells effectively suppresses the growth of glioma in rats. Cell biology international. 2009;33(4):466-74. Epub 2008/08/30.
50. Aboody KS, Najbauer J, Danks MK. Stem and progenitor cell-mediated tumor selective gene therapy. Gene therapy. 2008;15(10):739-52. Epub 2008/03/29.
51. Chen X, Lin X, Zhao J, Shi W, Zhang H, Wang Y, et al. A tumor-selective biotherapy with prolonged impact on established metastases based on cytokine gene-engineered MSCs. Molecular therapy : the journal of the American Society of Gene Therapy. 2008;16(4):749-56. Epub 2008/03/26.
52. Nakamura K, Ito Y, Kawano Y, Kurozumi K, Kobune M, Tsuda H, et al. Antitumor effect of genetically engineered mesenchymal stem cells in a rat glioma model. Gene therapy. 2004;11(14):1155-64. Epub 2004/05/14.

53. Manning E, Pham S, Li S, Vazquez-Padron RI, Mathew J, Ruiz P, et al. Interleukin-10 delivery via mesenchymal stem cells: a novel gene therapy approach to prevent lung ischemia-reperfusion injury. Human gene therapy. 2010;21(6):713-27. Epub 2010/01/28.
54. Vidal Vera P, Lemmens, E., Franscesco, B., Nelissen, S., Vangansewinkel, T., Hendrix, S. . IL-13 stimulates neurite outgrowth in primary neurons and organotypic brain slices. . Journal of Neuroimmunology. 2010;228:130.
55. Nelissen S, Boato, F., Lemmens, E., Nitsch, R., Hendrix, S. Il-4 and IL-13 exert opposing effects on functional recovery after spinal cord injury. Journal of Neuroimmunology. 2010;228:132.
56. Conti L, Pollard SM, Gorba T, Reitano E, Toselli M, Biella G, et al. Niche-independent symmetrical self-renewal of a mammalian tissue stem cell. PLoS biology. 2005;3(9):e283. Epub 2005/08/10.
57. Livak KJ, Schmittgen TD. Analysis of relative gene expression data using real-time quantitative PCR and the 2(-Delta Delta C(T)) Method. Methods. 2001;25(4):402-8. Epub 2002/02/16.
58. Boato F, Hendrix S, Huelsenbeck SC, Hofmann F, Grosse G, Djalali S, et al. C3 peptide enhances recovery from spinal cord injury by improved regenerative growth of descending fiber tracts. Journal of cell science. 2010;123(Pt 10):1652-62. Epub 2010/04/22.
59. Basso DM, Fisher LC, Anderson AJ, Jakeman LB, McTigue DM, Popovich PG. Basso Mouse Scale for locomotion detects differences in recovery after spinal cord injury in five common mouse strains. Journal of neurotrauma. 2006;23(5):635-59. Epub 2006/05/13.
60. Glaser T, Pollard SM, Smith A, Brustle O. Tripotential differentiation of adherently expandable neural stem (NS) cells. PloS one. 2007;2(3):e298. Epub 2007/03/16.
61. Sun Y, Pollard S, Conti L, Toselli M, Biella G, Parkin G, et al. Long-term tripotent differentiation capacity of human neural stem (NS) cells in adherent culture. Molecular and cellular neurosciences. 2008;38(2):245-58. Epub 2008/05/03.
62. McKay R. Stem cells in the central nervous system. Science. 1997;276(5309):66-71. Epub 1997/04/04.
63. Kota RS, Rutledge JC, Gohil K, Kumar A, Enelow RI, Ramana CV. Regulation of gene expression in RAW 264.7 macrophage cell line by interferon-gamma. Biochemical and biophysical research communications. 2006;342(4):1137-46. Epub 2006/03/07.
64. Perona-Wright G, Mohrs K, Mayer KD, Mohrs M. Differential regulation of IL-4Ralpha expression by antigen versus cytokine stimulation characterizes Th2 progression in vivo. J Immunol. 2010;184(2):615-23. Epub 2009/12/19.
65. da Silva AG, Campello-Costa P, Linden R, Sholl-Franco A. Interleukin-4 blocks proliferation of retinal progenitor cells and increases rod photoreceptor differentiation through distinct signaling pathways. J Neuroimmunol. 2008;196(1-2):82-93. Epub 2008/04/02.
66. Lin SJ, Chang C, Ng AK, Wang SH, Li JJ, Hu CP. Prevention of TGF-beta-induced apoptosis by interlukin-4 through Akt activation and p70S6K survival signaling pathways. Apoptosis : an international journal on programmed cell death. 2007;12(9):1659-70. Epub 2007/07/13.
67. Brodie C, Goldreich N, Haiman T, Kazimirsky G. Functional IL-4 receptors on mouse astrocytes: IL-4 inhibits astrocyte activation and induces NGF secretion. J Neuroimmunol. 1998;81(1-2):20-30. Epub 1998/04/01.
68. Sawada M, Itoh, Y., Suzumura, A., Marunouchi, T. Expression of cytokine receptors in cultured neuronal and glial cells. . Neuroscience letters. 1993;160:131-4.
69. Gouwy M, Struyf S, Proost P, Van Damme J. Synergy in cytokine and chemokine networks amplifies the inflammatory response. Cytokine & growth factor reviews. 2005;16(6):561-80. Epub 2005/07/19.
70. Ronsyn MW, Daans J, Spaepen G, Chatterjee S, Vermeulen K, D'Haese P, et al. Plasmid-based genetic modification of human bone marrow-derived stromal cells: analysis of cell survival and transgene expression after transplantation in rat spinal cord. BMC biotechnology. 2007;7:90. Epub 2007/12/15.

71. Hechler D, Nitsch R, Hendrix S. Green-fluorescent-protein-expressing mice as models for the study of axonal growth and regeneration in vitro. Brain research reviews. 2006;52(1):160-9. Epub 2006/02/25.
72. Limberis MP, Bell CL, Wilson JM. Identification of the murine firefly luciferase-specific CD8 T-cell epitopes. Gene therapy. 2009;16(3):441-7. Epub 2009/01/09.
73. Matrai J, Chuah MK, VandenDriessche T. Recent advances in lentiviral vector development and applications. Molecular therapy : the journal of the American Society of Gene Therapy. 2010;18(3):477-90. Epub 2010/01/21.
74. Epstein NE, Silvergleid RS, Hollingsworth R. Increased postoperative cervical myelopathy and cord compression resulting from the use of Gelfoam. The spine journal : official journal of the North American Spine Society. 2009;9(2):e19-21. Epub 2008/05/23.
75. Vaquero J, Zurita M, Oya S, Santos M. Cell therapy using bone marrow stromal cells in chronic paraplegic rats: systemic or local administration? Neuroscience letters. 2006;398(1-2):129-34. Epub 2006/01/21.
76. Jang CH, Park H, Cho YB, Choi CH. The effect of anti-adhesive packing agents in the middle ear of guinea pig. International journal of pediatric otorhinolaryngology. 2008;72(11):1603-8. Epub 2008/09/05.
77. Bottai D, Madaschi L, Di Giulio AM, Gorio A. Viability-dependent promoting action of adult neural precursors in spinal cord injury. Mol Med. 2008;14(9-10):634-44. Epub 2008/07/26.
78. Gwak YS, Kang J, Unabia GC, Hulsebosch CE. Spatial and temporal activation of spinal glial cells: role of gliopathy in central neuropathic pain following spinal cord injury in rats. Experimental neurology. 2012;234(2):362-72. Epub 2011/11/01.

# Supplemental information

## Supplemental results

### NSCs express A2B5, NCAM, GFAP, BLBP and SOX2, but are negative for CD45, Sca-1, Tuj1 and NeuN

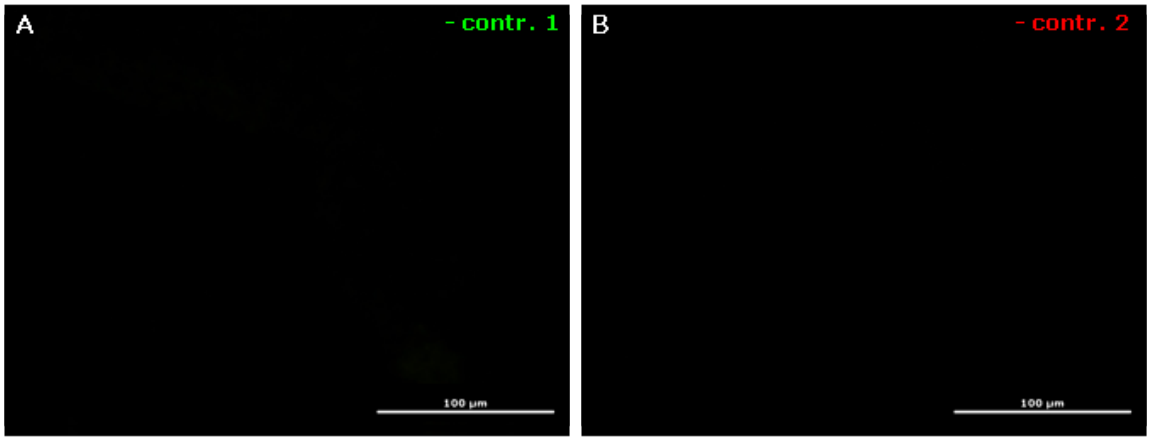


**Figure S1: Negative controls showed no non-specific binding of Alexa Fluor 488-labeled goat anti-rabbit secondary antibody and Alexa Fluor 568-labeled goat anti-mouse secondary antibody. A)** Negative control 1 (-contr. 1): NSCs only stained with the secondary anti-rabbit antibody (green). **B)** Negative control 2 (- contr. 2): NSCs only stained with the secondary anti-mouse antibody (red). The negative controls showed no signal. Scale bars: 100 µm, as indicated.

### NSCs have the capacity to differentiate into glial and neuronal cell lineages *in vitro*

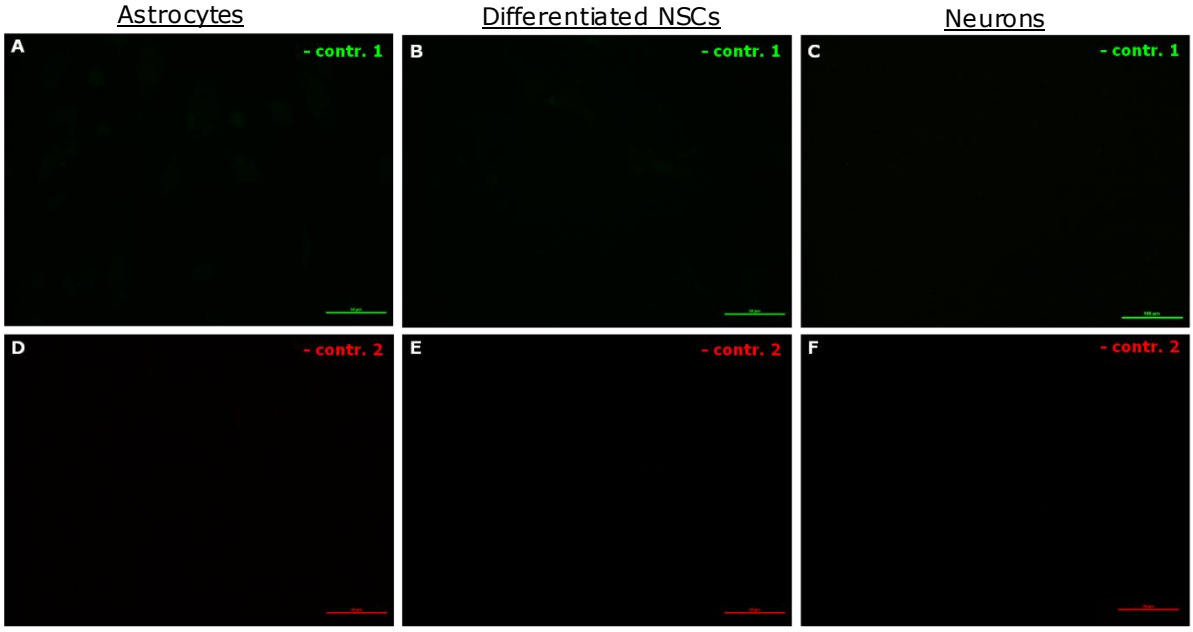


**Figure S2: Negative controls showed no non-specific binding of Alexa Fluor 488-labeled goat anti-rabbit secondary antibody and Alexa Fluor 568-labeled goat anti-mouse secondary antibody. A-C)** Negative control 1 (- contr. 1): Astrocytes (A), differentiated NSCs (B) and neurons (C) only stained with the secondary anti-rabbit antibody (green). **D-F)** Negative control 2 (- contr. 2): Astrocytes (A), differentiated NSCs (B) and neurons (C) only stained with the secondary anti-mouse antibody (red). The negative controls showed no signal. Scale bars: 50 µm, as indicated.

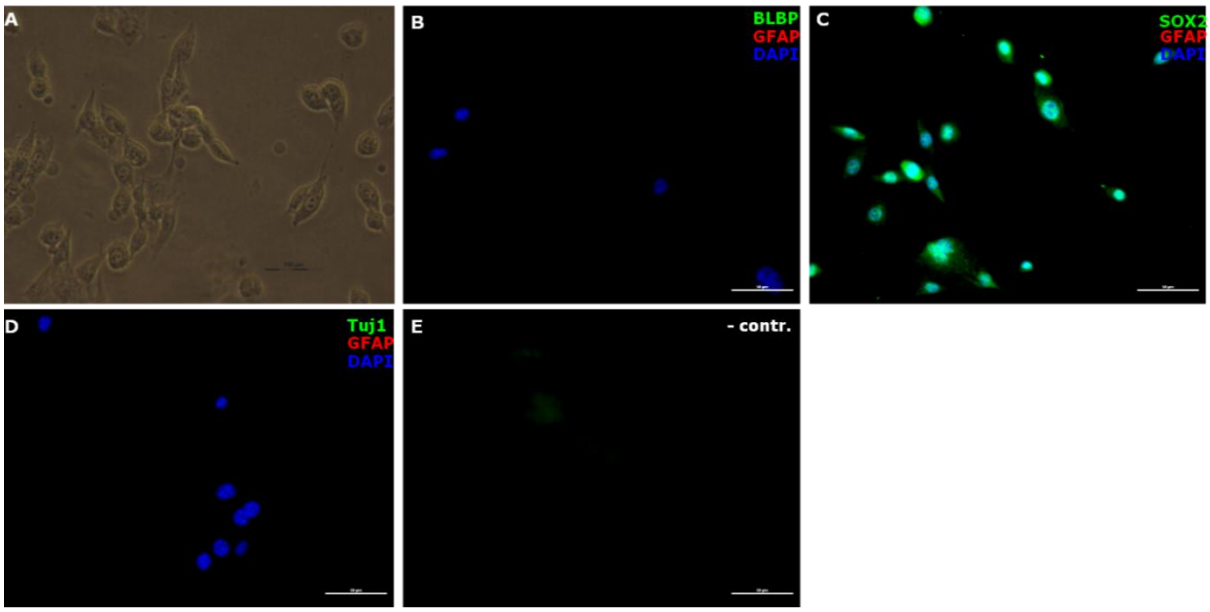


**Figure S3: The fibroblasts stained negative for the neural markers BLBP, GFAP and Tuj1, but positive for SOX2. A)** Bright field microscopy picture of the fibroblast culture. **B)** Immunofluorescence staining for BLBP (green) and GFAP (red). **C)** Immunofluorescence double staining for SOX2 (green) and GFAP (red). **D)** Double staining for Tuj1 (green) and GFAP (red). **E)** The negative control (- contr.) was double stained with only the secondary antibodies. There was no signal present, indicating no non-specific binding. DAPI (blue) was used as counter staining. GFAP, Glial fibrillary acidic protein; BLBP, Brain lipid binding protein; SOX2, sex determining region Y-box 2; Tuj1, neuron-specific beta3 tubulin; DAPI, 4',6-diamidino-2-phenylindole. Scale bars: 50 µm, as indicated.

**Real time-PCR suggests the expression of IL-13Rα1 on the NSCs after quantitative analysis and expression of IL-13Rα1 and IL-2Rγ after gel electrophoresis, however expression of IL-4Rα is also suggested after IL-4 treatment**

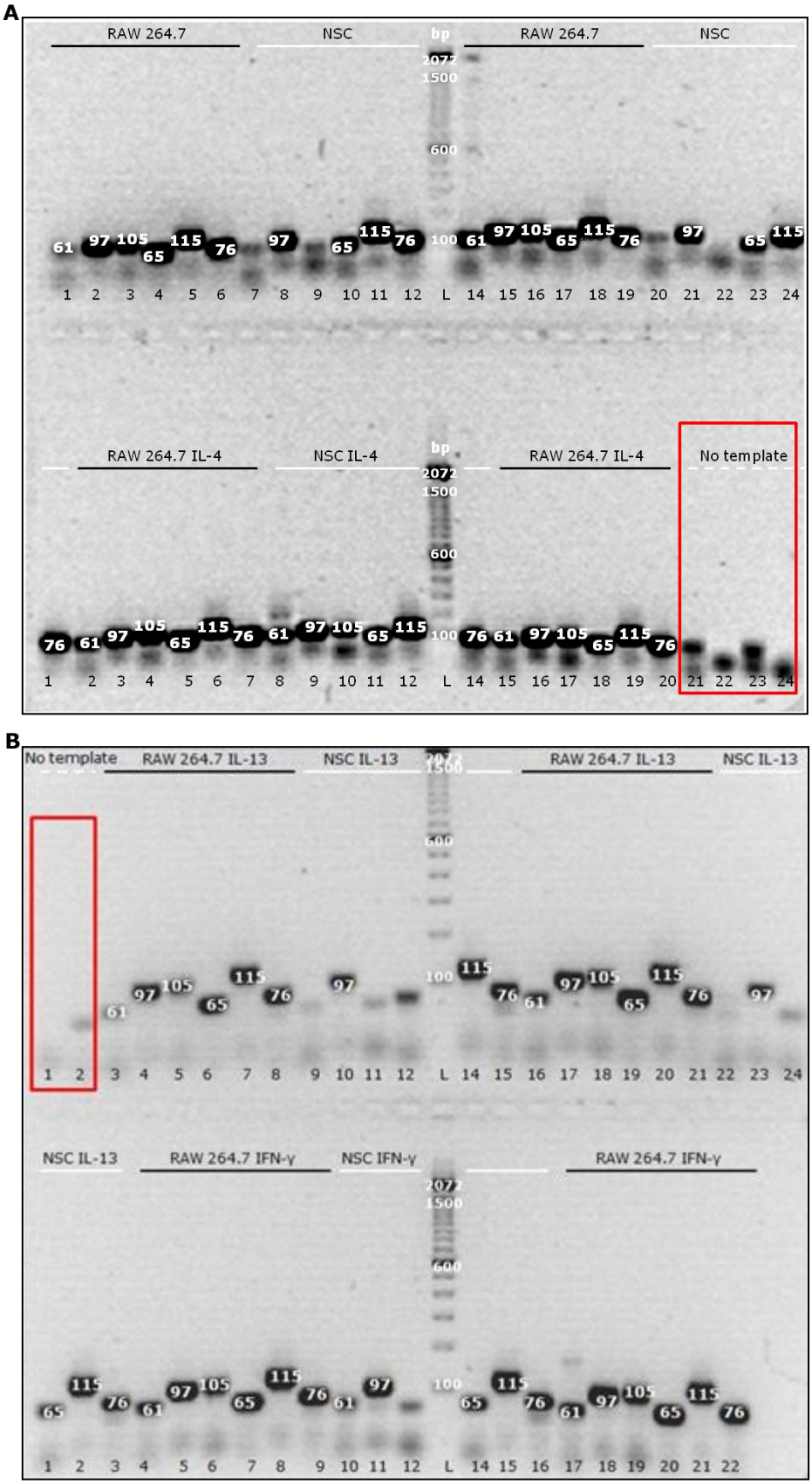

C

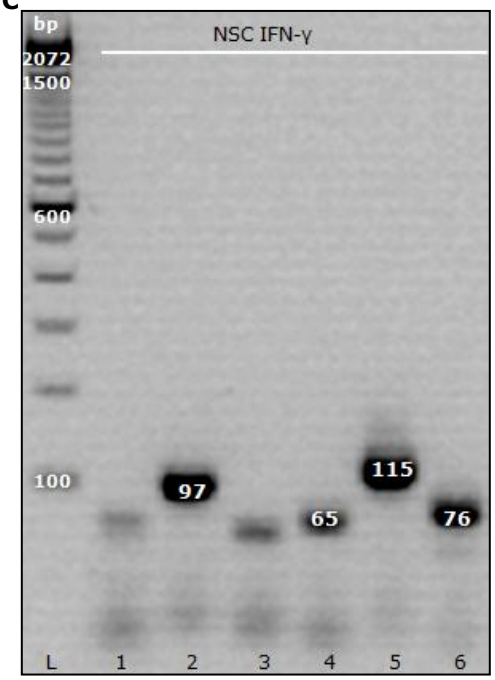


**Figure S4: Agarose gel electrophoresis showed the presence of amplicons for IL-13Rα1 and IL-2Rγ on the NSCs and the presence of all IL-4 receptor units after addition of IL-4. A) Gel 1**: The electrophoresis result of amplicons of the IL-4Rα (61 bp), IL-13Rα1 (97 bp), IL-13Rα2 (105 bp), IL-2Rγ (65 bp) receptor units, and B-actin (115 bp) and Gus-B (76 bp) for the RAW 264.7 cells (in duplo, lanes 1-6 and lanes 14-19) and NSCs (lanes 20-24) are presented. **Gel 2**: The electrophoresis result of amplicons of the IL-4Rα (61 bp), IL-13Rα1 (97 bp), IL-13Rα2 (105 bp), IL-2Rγ (65 bp), B-actin (115 bp), Gus-B (76 bp) receptor units for the NSCs (lane 1), IL-4 stimulated RAW 264.7 cells (in duplo, lanes 2-7 and lanes 15-20), IL-4 stimulated NSCs (lanes 8-14) and the no template control (lanes 21-24) is presented. The lanes discussed in the results section are indicated in the red box. **B) Gel 1**: The electrophoresis result of amplicons of the IL-4Rα (61 bp), IL-13Rα1 (97 bp), IL-13Rα2 (105 bp), IL-2Rγ (65 bp), B-actin (115 bp), Gus-B (76 bp) receptor units for the no template control (lanes 1 and 2), the IL-13 stimulated RAW 264.7 cells (in duplo, lanes 3-8 and lanes 16-20), IL-13 stimulated NSCs (in duplo, lanes 9-15 and lanes 22-24) is presented. **Gel 2**: IL-13 stimulated NSCs continued (lanes 1-3), IFN-γ stimulated RAW 264.7 cells (in duplo, lanes 4-9 and lanes 17-22), IFN-γ stimulated NSCs (lanes 10-16). The lanes discussed in the results section are indicated in the red box. **C)** The electrophoresis result of amplicons of the IL-4Rα (61 bp), IL-13Rα1 (97 bp), IL-13Rα2 (105 bp), IL-2Rγ (65 bp), B-actin (115 bp), Gus-B (76 bp) receptor units is presented for IFN-γ stimulated NSCs (lanes 1-6). This result is included for completeness. The L-lanes represent the 100 bp ladder.

## The NSCs show immunoreactivity for IL-13Rα1

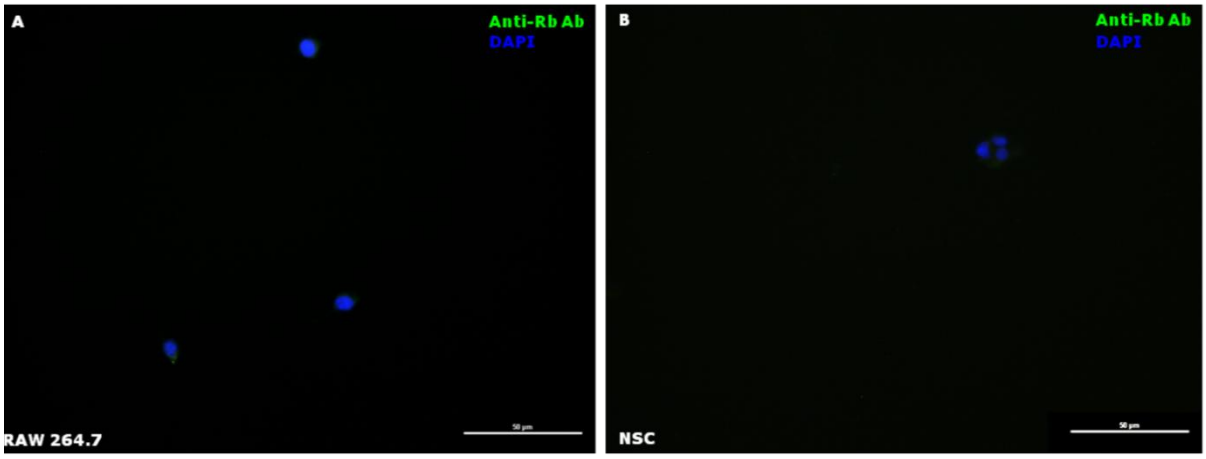


**Figure S5: The negative controls, only incubated with secondary antibodies, showed no non-specific staining. A-B)** Negative controls: RAW 264.7 cells and NSCs only incubated with secondary Alexa Fluor 488 labeled anti-rabbit antibody (Anti-Rb Ab). No signal was present. DAPI, 4',6-diamidino-2-phenylindole; NSC, Neural stem cell. Scale bars: 50 µm, as indicated.

## Histological analysis does not reveal the presence of transplanted BMSCs at the lesion site, three weeks after transplantation

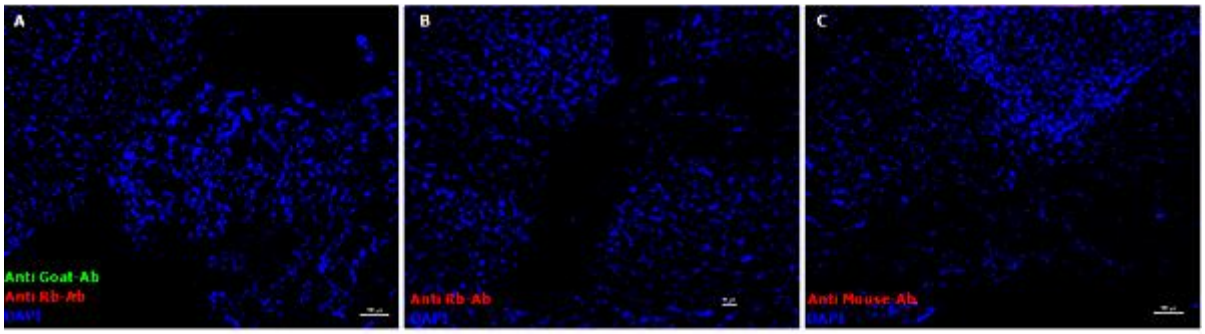


**Figure S6: Negative controls showed no non-specific binding of the Alexa Fluor 488-labeled donkey anti-goat, Alexa Fluor 555-labeled donkey anti-rabbit and Alexa Fluor 568-labeled goat anti-mouse secondary antibodies. A)** Negative control, used for the eGFP and Iba1 double staining of spinal cord tissue sections, only stained with the secondary anti-goat (green) and anti-rabbit (red) antibody, counterstained with DAPI (nucleus, blue). **B)** Negative control, used for the Iba1 staining of spinal cord tissue sections, only stained with the secondary anti-rabbit (red) antibody, counterstained with DAPI (nucleus, blue). **C)** Negative control, used for the GFAP-staining of spinal cord tissue section, only stained with the secondary anti-mouse antibody (red), counterstained with DAPI (nucleus, blue). The negative controls showed no signal. Scale bars: 50 µm and 100 µm, as indicated.

# Auteursrechtelijke overeenkomst

Ik/wij verlenen het wereldwijde auteursrecht voor de ingediende eindverhandeling:
**Using stem cells as carriers of IL-4 to promote recovery after spinal cord injury**

Richting: **master in de biomedische wetenschappen-klinische moleculaire wetenschappen**
Jaar: **2012**

in alle mogelijke mediaformaten, - bestaande en in de toekomst te ontwikkelen - , aan de Universiteit Hasselt.

Niet tegenstaand deze toekenning van het auteursrecht aan de Universiteit Hasselt behoud ik als auteur het recht om de eindverhandeling, - in zijn geheel of gedeeltelijk -, vrij te reproduceren, (her)publiceren of distribueren zonder de toelating te moeten verkrijgen van de Universiteit Hasselt.

Ik bevestig dat de eindverhandeling mijn origineel werk is, en dat ik het recht heb om de rechten te verlenen die in deze overeenkomst worden beschreven. Ik verklaar tevens dat de eindverhandeling, naar mijn weten, het auteursrecht van anderen niet overtreedt.

Ik verklaar tevens dat ik voor het materiaal in de eindverhandeling dat beschermd wordt door het auteursrecht, de nodige toelatingen heb verkregen zodat ik deze ook aan de Universiteit Hasselt kan overdragen en dat dit duidelijk in de tekst en inhoud van de eindverhandeling werd genotificeerd.

Universiteit Hasselt zal mij als auteur(s) van de eindverhandeling identificeren en zal geen wijzigingen aanbrengen aan de eindverhandeling, uitgezonderd deze toegelaten door deze overeenkomst.

Voor akkoord,

**Lemmens, Stefanie**

Datum: **11/06/2012**